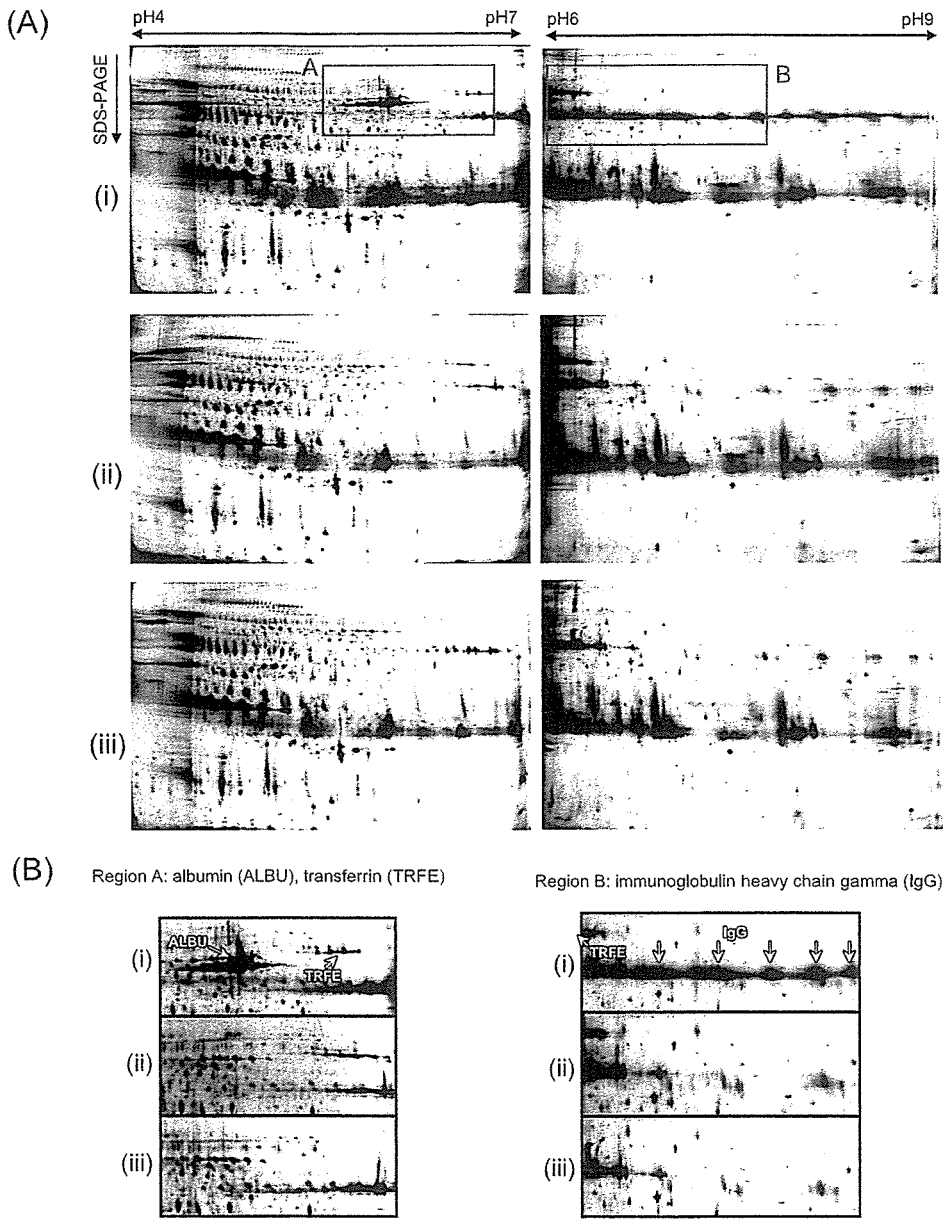

Fig. 6.　2-DE of urinary proteins after depletion of high-abundant proteins using different depletion columns.

(A) Urinary proteins were labeled with CyDye, and separated in the first dimension on pH 4–7 and 6–9 IPG strips and in the second dimension on a 10% polyacrylamide gel. (i) Crude samples; (ii) Albumin and IgG Removal Kit (GE Healthcare); (iii) MARS Cartridge (Agilent technologies). (B) Enlarged views of region A and B in 2-DE images.

CyDye にてラベルし，二次元電気泳動を行った．試験紙法にて尿タンパク陰性の尿では，ヒト血清を対象としている両者のカラム共にタンパク量の回収率は約 70% であった．Fig. 6 にカラム未使用の場合と，2 種のカラムで処理したそれぞれの泳動像を示す．タンパク質スポット数はカラム未使用と比して大きな変化はないものの Albumin と IgG のスポットは顕著に減少し，Albumin などにマスクされていたタンパク質スポットが検出可能となった．尿タンパク質を上述した方法にて処理することで，約 10 ml の尿から回収したタンパク質で二次元電気泳動が行うことができ，さらにアフィニティーカラムを用いた高含有量タンパク質の除去により，泳動のストリーキングを改善し，微量タンパク質の検出に有効であると考えられる．現在，以上の方法にて糖尿病患者尿の解析を行っている．

結　語

本研究室で行われている 2D DIGE を中心としたプロテオーム解析手法を用いた研究の一端を紹介した．本法は，同

一ゲル内で内部標準サンプルを同時に泳動することによって，サンプル間のタンパク質スポットの変動を厳密に評価することが可能であるため，糖尿病状態におけるタンパク質発現の微細な変化を検出することに適している．さらに，2D DIGE に本稿で示したような 1）多次元 LC-MS/MS を用いた網羅的タンパク質同定，2）細胞小器官（オルガネラ）レベルでのプロテオーム解析，3）質量分析器での翻訳後修飾部位同定といった手法を組み合わせることによって，新規の糖尿病治療ターゲット及び診断マーカーの検索に一層の有効性を発揮するものと考える．

文　献

1) Fasshauer M, Paschke R. Regulation of adipocytokines and insulin resistance. Diabetologia 2003;46:1594–1603.
2) Kadowaki T, Yamauchi T. Adiponectin and adiponectin receptors. Endocr Rev 2005;26:439–451.
3) Kratchmarova I, Kalume DE, Blagoev B, Scherer PE, Podtelejnikov AV, Molina H, Bickel PE, Andersen JS, Fernandez MM, Bunkenborg J, Roepstorff P, Kristiansen K, Lodish HF, Mann M, Pandey A. A proteomic approach for identification of secreted proteins during the differentiation of 3T3-L1 preadipocytes to adipocytes. Mol Cell Proteomics 2002;1:213–222.
4) Dupont A, Tokarski C, Dekeyzer O, Guihot AL. Two-dimensional maps and databases of the human macrophage proteome and secretome. Proteomics 2004;4:1761–1778.
5) Dupont A, Corseaux D, Dekeyzer O, Drobecq H, Guihot AL, Susen S, Vincentelli A, Amouyel P, Jude B, Pinet F. The proteome and secretome of human arterial smooth muscle cells. Proteomics 2005;5:585–596.
6) Chen X, Cushman SW, Pannell LK, Hess S. Quantitative proteomic analysis of the secretory proteins from rat adipose cells using a 2D liquid chromatography-MS/MS approach. J Proteome Res 2005;4:570–577.
7) Sanchez JC, Appel RD, Golaz O, Pasquali C, Ravier F, Bairoch A, Hochstrasser DF. Inside SWISS-2DPAGE database. Electrophoresis 1995;16:1131–1151.
8) Yamashita R, Saito T, Satoh S, Aoki K, Kaburagi Y, Sekihara H. Effects of dehydroepiandrosterone on gluconeogenic enzymes and glucose uptake in human hepatoma cell line, HepG2. Endocr J 2005;52:727–733.
9) Yamashita R, Yasuda K, Kaburagi Y. Proteomic analysis of proteins secreted from hepatocytes. J Mass Spetrom Soc Jpn 2005;3:164–168.
10) Volmer MW, Stuhler K, Zapatka M, Schoneck A, Klein-Scory S, Schmiegel W, Meyer HE, Schwarte-Waldhoff I. Differential proteome analysis of conditioned media to detect Smad4 regulated secreted biomarkers in colon cancer. Proteomics 2005;5:2587–2601.
11) Shimamura M, Matsuda M, Kobayashi S, Ando Y, Ono M, Koishi R, Furukawa H, Makishima M, Shimomura I. Angiopoietin-like protein 3, a hepatic secretory factor, activates lipolysis in adipocytes. Biochem Biophys Res Commun 2003;301:604–609.
12) DeFronzo RA, Ferrannini E. Insulin resistance. A multifaceted syndrome responsible for NIDDM, obesity, hypertension, dyslipidemia, and atherosclerotic cardiovascular disease. Diabetes Care 1991;14:173–194.
13) White MF. IRS proteins and the common path to diabetes. Am J Physiol Endocrinol Metab 2002;283:E413–E422.
14) Kaburagi Y, Satoh S, Tamemoto H, Yamamoto-Honda R, Tobe K, Ueki K, Yamauchi T, Kono-Sugita E, Sekihara H, Aizawa S, Cushman SW, Akanuma Y, Yazaki Y, Kadowaki T. Role of insulin receptor substrate-1 and pp60 in the regulation of insulin-induced glucose transport and GLUT4 translocation in primary adipocytes. J Biol Chem 1997;272:25839–25844.
15) Kaburagi Y, Satoh S, Yamamoto-Honda R, Ito Y, Akanuma Y, Sekihara H, Yasuda K, Sasazuki T, Kadowaki T, Yazaki Y. Protection of insulin receptor substrate-3 from staurosporine-induced apoptosis. Biochem Biophys Res Commun 2003;300:371–377.
16) Kaburagi Y, Yamashita R, Ito Y, Okochi H, Yamamoto-Honda R, Yasuda K, Sekihara H, Sasazuki T, Kadowaki T, Yazaki Y. Insulin-induced cell cycle progression is impaired in chinese hamster ovary cells overexpressing insulin receptor substrate-3. Endocrinology 2004;145:5862–5874.
17) Kaburagi Y, Satoh S, Yamamoto-Honda R, Ito T, Ueki K, Akanuma Y, Sekihara H, Kimura S, Kadowaki T. Insulin-independent and wortmannin-resistant targeting of IRS-3 to the plasma membrane via its pleckstrin homology domain mediates a different interaction with the insulin receptor from that of IRS-1. Diabetologia 2001;44:992–1004.
18) Caramori ML, Fioretto P, Mauer M. The need for early predictors of diabetic nephropathy risk: is albumin excretion rate sufficient? Diabetes 2000;49:1399–1408.
19) Gerstein HC, Mann JF, Yi Q, Zinman B, Dinneen SF, Hoogwerf B, Halle JP, Young J, Rashkow A, Joyce C, Nawaz S, Yusuf S; HOPE Study Investigators. Albuminuria and risk of cardiovascular events, death, and heart failure in diabetic and nondiabetic individuals. JAMA 2001;286:421–426.
20) Hillege HL, Fidler V, Diercks GF, van Gilst WH, de Zeeuw D, van Veldhuisen DJ, Gans RO, Janssen WM, Grobbee DE, de Jong PE; Prevention of Renal and Vascular End Stage Disease (PREVEND) Study Group. Urinary albumin excretion predicts cardiovascular and noncardiovascular mortality in general population. Circulation 2002;106:1777–1782.
21) Pieper R, Gatlin CL, McGrath AM, Makusky AJ, Mondal M, Seonarain M, Field E, Schatz CR, Estock MA, Ahmed N, Anderson NG, Steiner S. Characterization of the human urinary proteome: a method for high-resolution display of urinary proteins on two-dimensional electrophoresis gels with a yield of nearly 1400 distinct protein spots. Proteomics 2004;4:1159–1174.
22) Oh J, Pyo JH, Jo EH, Hwang SI, Kang SC, Jung JH, Park EK, Kim SY, Choi JY, Lim J. Establishment of a near-standard two-dimensional human urine proteomic map. Proteomics 2004;4:3485–3497.

23) Tantipaiboonwong P, Sinchaikul S, Sriyam S, Phutrakul S, Chen ST. Different techniques for urinary protein analysis of normal and lung cancer patients. Proteomics 2005;5:1140–1149.
24) Sharma K, Lee S, Han S, Lee S, Francos B, McCue P, Wassell R, Shaw MA, RamachandraRao SP. Two-dimensional fluorescence difference gel electrophoresis analysis of the urine proteome in human diabetic nephropathy. Proteomics 2005;5:2648–2655.

Minodronate Suppresses Prostaglandin F2α-induced Vascular Endothelial Growth Factor Synthesis in Osteoblasts

Y. Hanai[1,2]
H. Tokuda[1,2]
S. Takai[1]
A. Harada[3]
T. Ohta[4]
O. Kozawa[1]

Abstract

In our previous study, we showed that prostaglandin $F_{2\alpha}$ ($PGF_{2\alpha}$) stimulates vascular endothelial growth factor (VEGF) synthesis via activation of p44/p42 mitogen-activated protein (MAP) kinase via protein kinase C (PKC) in osteoblast-like MC3T3-E1 cells. In addition, we demonstrated that incadronate amplified, and tiludronate suppressed $PGF_{2\alpha}$-induced VEGF synthesis among bisphosphonates, while alendronate or etidronate had no effect. In the present study, we investigated the effects of minodronate, a newly developed bisphosphonate, on $PGF_{2\alpha}$-induced VEGF synthesis in MC3T3-E1 cells. Minodronate significantly reduced VEGF synthesis induced by $PGF_{2\alpha}$ dose-dependently at levels between 3 and 100 μM. $PGF_{2\alpha}$-stimulated phosphorylation of Raf-1, MEK1/2 and p44/p42 MAP kinase were suppressed by minodronate. 12-*O*-tetradecanoylphorbol-13-acetate (TPA), a direct activator VEGF synthesis induced by PKC, was inhibited by minodronate. Minodronate inhibited Raf-1, MEK1/2 and p44/p42 MAP kinase phosphorylation induced by TPA. Mevalonate failed to affect the suppressive effect of minodronate on $PGF_{2\alpha}$-induced VEGF synthesis. Taken together, these results indicate that minodronate suppresses $PGF_{2\alpha}$-stimulated VEGF synthesis at the point between PKC and Raf-1 in osteoblasts.

Key Words

Bisphosphonate · prostaglandin $F_{2\alpha}$ · vascular endothelial growth factor · osteoblast

Introduction

Osteoblasts and osteoclasts are main functional cells that regulate bone metabolism. The former is responsible for bone formation, and the latter for bone resorption [1]. Bone-remodeling results from this finely coordinated process of bone resorption by activated osteoclasts coupled with subsequent deposition of new matrix by osteoblasts. Several bone-resorptive agents such as parathyroid hormone and 1,25-$(OH)_2$ vitamin D_3 upregulate RANKL (receptor activator of nuclear factor κB ligand) expression by binding specific receptors on osteoblasts, suggesting that osteoblasts also play crucial roles in the regulation of bone resorption [2]. During these processes, capillary endothelial cells along with microvasculature with osteoblasts and osteoprogenitor cells, which locally proliferate and differentiate into osteoblasts, migrate into the resorption lacuna. Therefore, osteoblasts, osteoclasts and capillary endothelial cells cooperatively regulate bone metabolism in a closely coordinated fashion via humoral factors as well as by direct cell-to-cell contact [3].

Affiliation
[1] Department of Pharmacology, Gifu University Graduate School of Medicine, Gifu, Japan
[2] Department of Clinical Laboratory, National Hospital for Geriatric Medicine, National Center for Geriatrics and Gerontology, Aichi, Japan
[3] Functional Restoration, National Hospital for Geriatric Medicine, National Center for Geriatrics and Gerontology, Aichi, Japan
[4] Internal Medicine, National Hospital for Geriatric Medicine, National Center for Geriatrics and Gerontology, Aichi, Japan

Correspondence
Osamu Kozawa · Department of Pharmacology · Gifu University Graduate School of Medicine · 1-1 Yanagido · Gifu 501-1194 · Japan · Phone: +81 (58) 230-6214 · Fax: +81 (58) 230-6215 · E-Mail: okozawa@cc.gifu-u.ac.jp

Received 12 July 2005 · **Accepted after revision** 7 December 2005

Bibliography
Horm Metab Res 2006; 38: 152–158 © Georg Thieme Verlag KG Stuttgart · New York ·
DOI 10.1055/s-2006-925177 · ISSN 0018-5043

Bisphosphonate, a stable analogue of pyrophosphate, is generally known as an inhibitor of bone resorption [4]. Bisphosphonates are widely used as a potent agent for the treatment of various metabolic bone diseases associated with increased osteoclastic bone resorption such as Paget's disease, tumoral bone disease, and osteoporosis [4]. Osteoclast recruitment, osteoclastic adhesion to bone surface and osteoclast activity inhibition is known to be the main mechanisms by which bisphosphonates inhibit bone resorptive actions [4]. In addition to osteoclasts, the inhibitory action of bisphosphonates on osteoclasts is reportedly partly mediated through its actions on osteoblasts [5,6]. In osteoblastic cell line CRP 10/30, both ibandronate and alendronate induce the synthesis of an osteoclastic bone resorption inhibitor [7]. In a previous study [8], we reported that tiludronate inhibits interleukin (IL)-6 synthesis in osteoblast-like MC3T3-E1 cells. Etidronate, alendronate, pamidronate and olpadronate prevent apoptosis of murine primary cultured osteoblasts via activation of p44/p42 mitogen-activated protein (MAP) kinase [9]. In cultured human fetal osteoblasts, pamidronate and zoledronate enhance differentiation and bone-forming activities [10]. Pamidronate and zoledronate also reportedly increase mRNA expression for osteoprotegerin in primary human osteoblasts [11]. In UMR-106-01 osteosarcoma cells, pamidronate and clodronate decrease receptor activator of nuclear factor κB ligand (RANKL) [12]. In addition, zoledronate upregulates osteocalcin and bone morphogenetic protein-2 (BMP-2) gene expression in human osteoblast-like cells [13], and decreases membrane RANKL expression by upregulating tumor necrosis factor-α-converting enzyme [14]. These studies led us to speculate that the effects of bisphosphonates on bone metabolism are not only exerted by osteoclasts, but also by osteoblasts. However, the detailed mechanism of bisphosphonate action on osteoblasts has not yet been fully clarified.

Vascular endothelial growth factor (VEGF) is a potent angiogenic factor that induces angiogenesis, endothelial cell proliferation and capillary permeability [15]. Inactivation of VEGF results in the complete suppression of vascular invasion followed by impaired trabecular bone formation and expansion of the hypertrophic chondrocyte zone in the mouse tibial epiphyseal growth plate [16]. Osteoblasts have been reported to produce and secrete VEGF in response to various physiological agonists [15,17]. In our previous studies, we reported that prostaglandin $F_{2\alpha}$ ($PGF_{2\alpha}$), a potent bone resorptive agent, activates both phosphoinositide (PI)-hydrolyzing phospholipase C (PI-phospholipase C) and phosphatidylcholine (PC)-hydrolyzing phospholipase D (PC-phospholipase D) [18,19], recognized as two major physiological protein kinase C (PKC) activation pathways [20,21], in osteoblast-like MC3T3-E1 cells. In addition, we recently showed that $PGF_{2\alpha}$ induces VEGF synthesis and secretion through PKC-dependent activation of p44/p42 MAP kinase in these cells [22]. Furthermore, we have demonstrated that incadronate enhances [22], while tiludronate suppresses [23] $PGF_{2\alpha}$-induced VEGF synthesis through activation [22] or suppression [23] of p44/p42 MAP kinase in osteoblast-like MC3T3-E1 cells, while alendronate or etidronate has little effect [22].

In the present study, we investigated the effect of minodronate, a newly developed nitrogen-containing bisphosphonate, which is structurally different and has a different side chain structure from incadronate, alendronate tiludronate or etidronate, on $PGF_{2\alpha}$-stimulated VEGF synthesis in MC3T3-E1 cells and the mechanism behind it. In contrast to the results from incadronate [22], and identical to those from tiludronate [22], this study will demonstrate that minodronate inhibits $PGF_{2\alpha}$-stimulated VEGF synthesis in these cells, and that the suppressive effect of minodronate is exerted at the point between PKC and Raf-1.

Materials and Methods

Materials

Minodronate was kindly provided by Yamanouchi Pharmaceuticals Co. Ltd. (Tokyo, Japan). $PGF_{2\alpha}$, 12-*O*-tetradecanoylphorbol-13-acetate (TPA) and mevalonate were purchased from Sigma Chemical Co. (St. Louis, MO). Phosphospecific p44/p42 MAP kinase antibodies, p44/p42 MAP kinase antibodies, phosphospecific MEK1/2 antibodies, MEK1/2 antibodies, phosphospecific Raf-1 antibodies and β-actin antibodies were purchased from New England Biolabs, Inc. (Beverly, MA). ECL Western blotting detection system was purchased from Amersham Japan (Tokyo, Japan). Mouse VEGF ELISA kit was purchased from R&D Systems, Inc. (Minneapolis, MN). Other materials and chemicals were obtained from Sigma Chemical Co. (St. Louis, MO) or Nacalai Tesque, Inc. (Kyoto, Japan). $PGF_{2\alpha}$ was dissolved in ethanol. TPA was dissolved in dimethyl sulfoxide. The maximum concentration of ethanol or dimethyl sulfoxide was 0.1%, which did not affect VEGF assay or Western blot analysis.

Cell culture

MC3T3-E1 cells are a clonal osteoblastic cell line derived from newborn mouse calvaria [24], and reportedly form mineralized matrix. In addition, we previously reported that MC3T3-E1 cells secrete osteocalcin [25] and express alkaline phosphatase [26] under our experimental conditions. MC3T3-E1 cells were maintained as previously described [27]. The cells were cultured in α-minimum essential medium (α-MEM) containing 10% fetal calf serum (FCS) at 37 °C in a humidified atmosphere of 5% CO_2/95% air. The cells were seeded into 35 mm (5×10^4) or 90 mm (2×10^5) diameter dishes in α-MEM containing 10% FCS. After five days, the medium was exchanged for α-MEM containing 0.3% FCS. The cells were used for experiments after 48 h.

Assay for VEGF

The cells were pretreated with various doses of minodronate or vehicle for 8 h, then stimulated by $PGF_{2\alpha}$ or TPA in 1 ml of α-MEM containing 0.3% FCS for the indicated period. In addition, mevalonate was added 8 h prior to stimulation by $PGF_{2\alpha}$ to investigate the involvement of mevalonate pathway on minodronate inhibition of VEGF synthesis by $PGF_{2\alpha}$. The conditioned medium was collected, and VEGF in the medium was measured by VEGF ELISA kit.

Analysis of p44/p42 MAP kinase, MEK1/2 or Raf-1

The cultured cells were pretreated with various doses of minodronate or vehicle for 8 h, then stimulated by $PGF_{2\alpha}$ or TPA in 4 ml of α-MEM containing 0.3% FCS for the indicated period. The cells were washed twice with phosphate-buffered saline and then lysed, homogenized and sonicated in a lysis buffer containing 62.5 mM Tris/HCl, pH 6.8, 2% sodium dodecyl sulfate

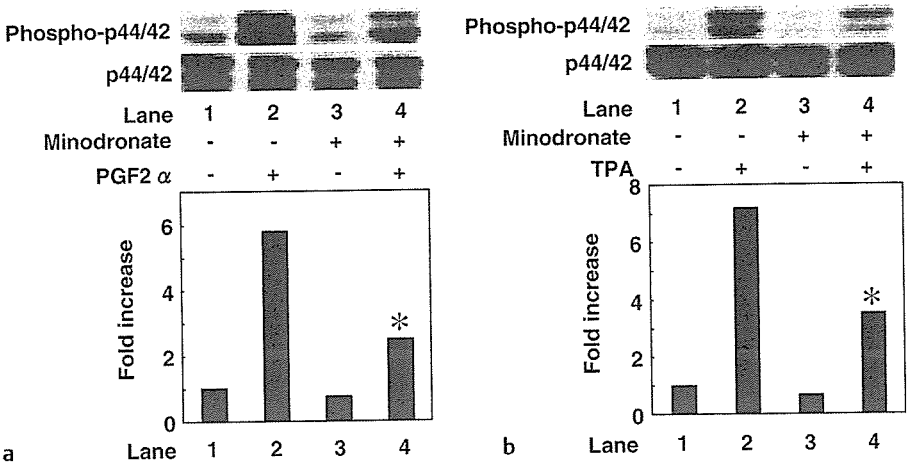

Fig. 1 Effects of minodronate on phosphorylation of p44/p42 MAP kinase induced by PGF2α or TPA in MC3T3-E1 cells. **a** Cultured cells were pretreated with 10 μM minodronate or vehicle for 8 h, then stimulated by 10 μM PGF2α or vehicle for 30 min. **b** The cultured cells were pretreated with 10 μM minodronate or vehicle for 8 h, and then stimulated by 0.1 μM TPA or vehicle for 60 min. Extracts of cells were subjected to SDS-PAGE with subsequent Western blot analysis using antibodies against phospho-specific p44/p42 MAP kinase or p44/p42 MAP kinase. The histogram shows quantitative representations of p44/p42 MAP kinase phosphorylation obtained from laser densitometric analysis. Each value represents the mean of triplicate determinations. Similar results were obtained with two additional and different cell preparations. *$p < 0.05$ compared to the value of PGF2α alone or TPA alone.

(SDS), 50 mM dithiothreitol, and 10% glycerol. SDS-PAGE was performed as described by Laemmli [28] in 10% polyacrylamide gel. Western blotting analysis was performed as described previously [29] using phosphospecific p44/p42 MAP kinase antibodies, p44/p42 MAP kinase antibodies, phosphospecific MEK1/2 antibodies, MEK1/2 antibodies, phosphospecific Raf-1 antibodies or β-actin antibodies, with peroxidase-labeled antibodies raised in goat anti-rabbit IgG used as second antibodies. Peroxidase activity on the nitrocellulose sheet was visualized on x-ray film using the ECL Western blotting detection system.

Determination of absorbance and densitometric analysis

Absorbance of ELISA samples was measured at 450 nm with a microplate spectrophotometer (Bio-Rad Laboratories, Hercules, CA). Densitometric analysis was performed using scanner and image analysis software (image J version 1.32).

Statistical analysis

Data were analyzed by ANOVA followed by Bonferroni's method for multiple comparisons between pairs, and values of $p < 0.05$ were considered significant. All data are presented as the mean ± SD from triplicate determinations. Each experiment was repeated three times with similar results.

Results

Effect of minodronate on PGF2α-induced VEGF synthesis in MC3T3-E1 cells

Recently, we have reported that $PGF_{2\alpha}$ induces VEGF synthesis in osteoblast-like MC3T3-E1 cells, and that incadronate amplifies VEGF synthesis while alendronate fails to affect synthesis [22]. Thus, we investigated the effect of minodronate on $PGF_{2\alpha}$-induced VEGF synthesis in these cells. Minodronate alone had little affect on VEGF levels, but significantly suppressed $PGF_{2\alpha}$-induced VEGF synthesis in MC3T3-E1 cells (49.1 ± 1.2 pg/ml for control; 33.1 ± 2.5pg/ml for 10μM minodronate alone, 1142.7 ± 186.5 pg/ml for 10μM $PGF_{2\alpha}$ alone; and 67.0 ± 5.5* pg/ml for 10 μM $PGF_{2\alpha}$ with 10 μM minodronate pretreatment, as measured during stimulation for 48 h; *$p < 0.05$, compared with the value of $PGF_{2\alpha}$ alone). The inhibitory effect of minodronate was dose-dependent between 3 and 100 μM (data not shown). Minodronate almost completely inhibited the $PGF_{2\alpha}$ effect at a dose of 10 μM. We confirmed that the cell number changed little by treatment [$(8.1 \pm 0.2) \times 10^5$ cells before incubation; $(7.9 \pm 0.4) \times 10^5$ cells after 48 h incubation with 100 μM minodronate; $(8.0 \pm 0.3) \times 10^5$ cells after 48 h incubation with vehicle].

Effects of minodronate on PGF2α-induced or TPA-induced phosphorylation of p44/p42 MAP kinase in MC3T3-E1 cells

In a previous study, we have demonstrated that $PGF_{2\alpha}$-induced VEGF synthesis is activated via p44/p42 MAP kinase in a PKC-dependent manner in MC3T3-E1 cells [22]. Therefore, we then investigated the detailed mechanism of minodronate underlying the inhibition of VEGF synthesis. Minodronate, which alone had little effect on phosphorylation of p44/p42 MAP kinase, markedly suppressed $PGF_{2\alpha}$-induced p44/p42 MAP kinase phosphorylation (Fig. **1 a**). According to densitometric analysis, minodronate (10 μM) caused a reduction of approximately 65% in the $PGF_{2\alpha}$ effect (*$p < 0.05$, compared with the value of $PGF_{2\alpha}$ alone).

To elucidate whether or not the effect of minodronate is exerted at a point downstream of PKC, we examined the effect of minodronate on phosphorylation of p44/p42 MAP kinase induced by TPA, a direct activator of PKC [30]. Previously, we found that p44/p42 MAP kinase was markedly phosphorylated by TPA by itself [31]. Minodronate significantly reduced p44/p42 MAP kinase phosphorylation stimulated by TPA (Fig. **1 b**). According to densitometric analysis, minodronate (10 μM) caused approximately 60% reduction in TPA effect (*$p < 0.05$, compared with the value of TPA alone).

Effect of minodronate on TPA-induced VEGF synthesis in MC3T3-E1 cells

Previously, we reported that TPA alone stimulated VEGF synthesis in osteoblast-like MC3T3-E1 cells [22]. Therefore, we investigated the effect of minodronate on TPA-induced VEGF synthesis. Minodronate significantly reduced TPA-induced syn-

Table 1 Effect of mevalonate minodronate on the TPA-induced VEGF synthesis in MC3T3-E1 cells

Minodronate	*TPA*	*VEGF (pg/ml)*
–	–	16 ± 3
–	+	280 ± 25
+	–	13 ± 2
+	+	59 ± 10*

Cultured cells were pretreated with 30 μM minodronate or vehicle for 8 h, then stimulated by 0.1 μM TPA or vehicle for 48 h. Cell viability after treatment was more than 90% of control cells. Each value represents the mean ± SD of triplicate determinations. Similar results were obtained with two additional and different cell preparations. *$p < 0.05$ compared to the value of TPA alone.

thesis of VEGF (Table 1). Minodronate (30 μM) caused a reduction of approximately 80% in TPA effect (*$p < 0.05$, compared with the value of TPA alone).

Effects of minodronate on phosphorylation of MEK1/2 induced by PGF2α or TPA in MC3T3-E1 cells

Activation of p44/p42 MAP kinase is known to be regulated by MEK1/2 as a MAP kinase kinase, which is regulated by an upstream kinase known as Raf-1 [32]. We have previously found that $PGF_{2\alpha}$ or TPA stimulates phosphorylation of both MEK1/2 and Raf-1 in osteoblast-like MC3T3-E1 cells [22]. Thus, we next examined the effect of minodronate on phosphorylation of MEK1/2 induced by $PGF_{2\alpha}$. Minodronate, which alone did not affect phosphorylation of MEK1/2, significantly suppressed $PGF_{2\alpha}$ induced MEK1/2 phosphorylation (Fig. 2a, *$p < 0.05$, compared with the value of $PGF_{2\alpha}$ alone). In addition, TPA-induced phos-

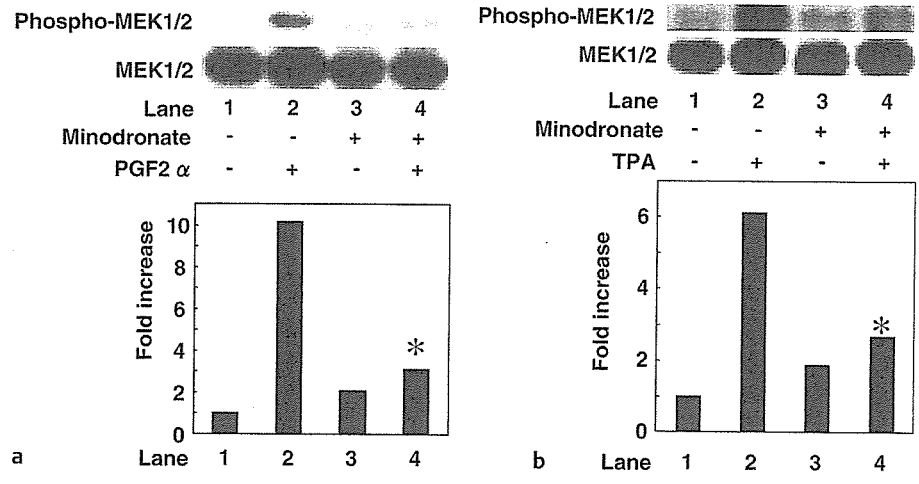

Fig. 2 Effects of minodronate on phosphorylation of MEK1/2 induced by PGF2α or TPA in MC3T3-E1 cells. (A) Cultured cells were pretreated with 10 μM minodronate or vehicle for 8 h, then stimulated by 10 μM $PGF_{2\alpha}$ or vehicle for 30 min. (B) The cultured cells were pretreated with 10 μM minodronate or vehicle for 8 h, then stimulated by 0.1 μM TPA or vehicle for 60 min. Extracts of cells were subjected to SDS-PAGE with subsequent Western blot analysis using antibodies against phosphospecific MEK1/2 or MEK1/2. The histogram shows quantitative representations of MEK1/2 phosphorylation obtained from laser densitometric analysis. Each value represents the mean of triplicate determinations. Similar results were obtained with two additional and different cell preparations. *$p < 0.05$, compared to the value of $PGF_{2\alpha}$ alone or TPA alone.

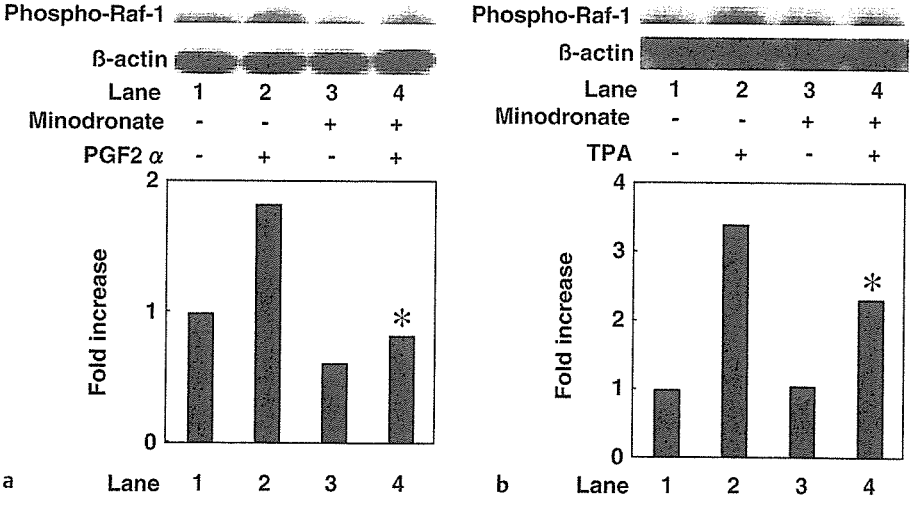

Fig. 3 Effects of minodronate on phosphorylation of Raf-1 induced by PGF2α or TPA in MC3T3-E1 cells. (**a**) The cultured cells were pretreated with 10 μM minodronate or vehicle for 8 h, then stimulated by 10 μM $PGF_{2\alpha}$ or vehicle for 15 min. (**b**) The cultured cells were pretreated with 10 μM minodronate or vehicle for 8 h, then stimulated by 0.1 μM TPA or vehicle for 60 min. Extracts of cells were subjected to SDS-PAGE with subsequent Western blot analysis using antibodies against phosphospecific Raf-1 or β-actin. The histogram shows quantitative representations of MEK1/2 phosphorylation obtained from laser densitometric analysis. Each value represents the mean of triplicate determinations. Similar results were obtained with two additional and different cell preparations. *$p < 0.05$ compared to the value of $PGF_{2\alpha}$ alone or TPA alone.

Table 2 Effect of mevalonate on minodronate inhibition of PGF2α-induced VEGF synthesis in osteoblast-like MC3T3-E1 cells

Minodronate	*Mevalonate*	*PGF2α*	*VEGF (pg/ml)*
–	–	–	33.0 ± 4.4
–	–	+	1095.0 ± 78.0
–	+	–	26.0 ± 4.5
–	+	+	1188.0 ± 282.1
+	–	–	16.0 ± 3.4
+	–	+	94.7 ± 4.2*
+	+	–	17.0 ± 3.5
+	+	+	81.3 ± 4.5*

Cultured cells were pretreated with 10 μM minodronate, 10 μM mevalonate or vehicle for 8 h, then stimulated by 10 μM $PGF_{2\alpha}$ or vehicle for 48 h. The cell viability after the treatments was more than 90% of control cells. Each value represents the mean ± SD of triplicate determinations. Similar results were obtained with two additional and different cell preparations. *$p < 0.05$, compared to the value of $PGF_{2\alpha}$ alone.

phorylation of MEK1/2 was markedly attenuated (Fig. **2b**, *$p < 0.05$, compared with the value of TPA alone).

Effects of minodronate on phosphorylation of Raf-1 induced by PGF2α or TPA in MC3T3-E1 cells

Previously, we reported that $PGF_{2\alpha}$ or TPA stimulated phosphorylation of Raf-1 in osteoblast-like MC3T3-E1 cells [22]. To clarify whether the effect of minodronate is exerted at a point upstream of Raf-1 or not, we examined the effect of minodronate on phosphorylation of Raf-1 induced by $PGF_{2\alpha}$ or TPA. Minodronate by itself did not affect Raf-1 phosphorylation, but significantly reduced phosphorylation of Raf-1 induced by $PGF_{2\alpha}$ (Fig. **3a**) or TPA (Fig. **3b**) (*$p < 0.05$, compared with the value of $PGF_{2\alpha}$ alone or TPA alone). According to densitometric analysis, minodronate (10 μM) caused a reduction of approximately 60% in the effect of $PGF_{2\alpha}$.

Effects of mevalonate on minodronate inhibition of PGF2α-induced VEGF synthesis in MC3T3-E1 cells

To clarify whether the mevalonate pathway is involved in minodronate inhibition of VEGF synthesis by $PGF_{2\alpha}$, we investigated the effect of mevalonate on the inhibition of VEGF synthesis by $PGF_{2\alpha}$ in MC3T3-E1 cells. Mevalonate, which alone had no effect on VEGF levels, did not affect either VEGF synthesis induced by $PGF_{2\alpha}$ or minodronate inhibition of $PGF_{2\alpha}$-induced VEGF synthesis (Table **2**).

Discussion

In contrast to the inhibitory effect of minodronate presented here, we have recently reported that incadronate, a nitrogen-containing bisphosphonate, but not alendronate enhances VEGF synthesis induced by $PGF_{2\alpha}$ in osteoblast-like MC3T3-E1 cells [22]. In contrast, we have recently reported that non-amino-bisphosphonate tiludronate, but not etidronate, inhibits $PGF_{2\alpha}$-induced VEGF release [23]. Thus, these findings suggest that the effects of bisphosphonates on $PGF_{2\alpha}$-induced VEGF synthesis in osteoblasts are compound-specific and vary among bisphosphonates. Pamidronate and zoledronate reportedly induce avascular necrosis of the jaw in a clinical setting [33,34], but no other bisphosphonates – including tiludronate and etidronate – are associated with avascular necrosis [33]. Taken together, the specific effects of each agent may be involved in clinical applications, supporting our present findings showing the agent-specific effects of bisphosphonates.

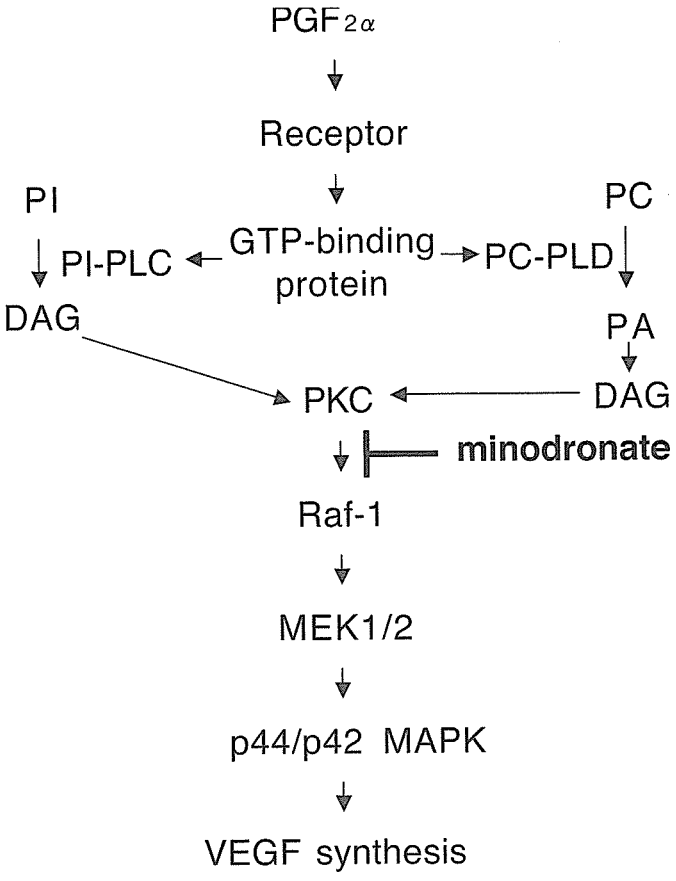

Fig. 4 Potential mechanisms in minodronate suppression of PGF2α-induced VEGF synthesis in MC3T3-E1 cells. GTP-binding protein, heterotrimeric GTP-binding protein; PI-PLC, phosphoinositide-hydrolyzing phospholipase C; PC-PLD, phosphatidylcholine-hydrolyzing phospholipase D,; PA, phosphatidic acid; DAG, diacylglycerol; PKC, protein kinase C; MAPK, mitogen-activated protein kinase; VEGF, vascular endothelial growth factor.

We previously reported that $PGF_{2\alpha}$ activated both PI-phospholipase C and PC-phospholipase D via heterotrimeric GTP-binding protein in osteoblast-like MC3T3-E1 cells [18,19], and also that $PGF_{2\alpha}$ activated p44/p42 MAP kinase in a PKC-dependent manner in these cells [35]. PI hydrolysis by phospholipase C and PC hydrolysis by phospholipase D are recognized as two major PKC-activating pathways [20,21]. In addition, we reported that $PGF_{2\alpha}$-induced VEGF synthesis through PKC-dependent, and probably PKCβI-dependent activation of p44/p42 MAP kinase in MC3T3-E1 cells [22]. Thus, we investigated the mechanism of minodronate underlying the inhibition of $PGF_{2\alpha}$-induced VEGF synthesis.

It is generally recognized that p44/p42 MAP kinase is activated through phosphorylation of threonine and tyrosine residues by dual-specificity MAP kinase kinase, known as MEK1/2 [32]. MEK1/2 is known to be activated by its own phosphorylation in-

duced by MAP kinase kinase kinase, Raf-1 [32]. We have demonstrated that minodronate also suppresses $PGF_{2\alpha}$ or TPA-induced phosphorylation of MEK1/2 and Raf-1. Taking our results as a whole, it is most likely that minodronate exerts its suppressive effect at the point between PKC and Raf-1 in $PGF_{2\alpha}$-stimulated VEGF synthesis in osteoblast-like MC3T3-E1 cells (Fig. **4**).

In the previous study, we reported that incadronate enhanced [22], while tiludronate suppressed [23] $PGF_{2\alpha}$-induced VEGF synthesis in MC3T3-E1 cells. Interestingly, the amplifying and suppressive effects of incadronate and tiludronate are exerted at a point between PKC and Raf-1 [22,23], where minodronate also showed suppressive effect in the present study. These findings suggest the different molecular mechanisms among the actions of bisphosphonates on osteoblasts, most likely their structural differences. There are considerable structural differences among these agents at the R2 side chain. Minodronate possesses 1-hydroxy-2-imidazo-(1, 2-a) pyridin-3-ylethylidene structure, and incadronate possess cycloheptylaminomethylene and 1-hydroxyethylidene structures [4], and tiludronate possesses (4-chlorophenyl) thiolmethylene structure with a more simple non-nitrogen-containing R2 side chain. In addition, the different effects of these bisphosphonates on VEGF synthesis may be related to their relative potency on anti-bone resorptive activities in these agents. In metabolic bone diseases, bone remodeling rates vary from case to case. To clarify the unique agent-specific effect(s) among bisphosphonates, it may be possible to select bisphosphonates according to the specific effect on bone-forming cells in adequate therapy by these drugs. Our present data together with our previous studies [22,23] would provide a new insight into the differences in pharmacological effects among bisphosphonates possibly due to their structural differences at the R2 side chain. Further investigation would be required to clarify the exact mechanism of bisphosphonate action on bone cells.

Nitrogen-containing bisphosphonates including minodronate are known to affect the mevalonate pathway and inhibit farnesyl diphosphate synthase [4]. We found that mevalonate did not affect the suppressive effect of minodronate on VEGF synthesis by $PGF_{2\alpha}$ in MC3T3-E1 cells. Therefore, it seems unlikely that mevalonate pathway is involved in the suppressive effect of minodronate on VEGF synthesis by $PGF_{2\alpha}$ in osteoblast-like MC3T3-E1 cells. In the present study, the effect of minodronate was significant at considerably higher doses than in clinical use. According to pharmacokinetic studies on bisphosphonates, these agents mainly accumulate in bone tissue *in vivo*[4]. Minodronate concentrations in the region probably reach much higher levels than do serum concentrations. Therefore, it is possible that the effect of minodronate shown here might be implicated in clinical relevance.

In conclusion, our present data strongly suggest that minodronate suppresses VEGF synthesis stimulated by $PGF_{2\alpha}$ in osteoblasts, and the inhibitory effect is exerted at the point between PKC and Raf-1.

Acknowledgments

This work was supported in part by a grant-in-aid for scientific research (16590873, 16591482) from the Ministry of Education, Science, Sports and Culture of Japan and research grants for longevity sciences (15A-1 and 15C-2) and health and labor sciences research grant for research on proteomics from the Ministry of Health, Labor and Welfare of Japan. The authors are very grateful to Mrs. S. Sakakibara for her skillful secretarial assistance.

References

[1] Nijweide PJ, Burger EH, Feyen JHM. Cells of bone: Proliferation, differentiation and hormonal regulation. Physiol Rev 1986; 66: 855–886

[2] Suda T, Takahashi N, Udagawa N, Jimi E, Gillespie MT, Martin TJ. Modulation of osteoclast differentiation and function by the new members of the tumor necrosis factor receptor and ligand families. Endocrine Rev 1999; 20: 345–357

[3] Erlebacher A, Filvaroff EH, Girelman SE, Derynck R. Toward a molecular understanding of skeletal development. Cell 1995; 80: 371–378

[4] Fleisch H, Reszka A, Rodan GA, Rogers M. Bisphosphonates. In: Bilezikian JP, Ratsz LG, Rodan GA (eds). Principles of Bone Biology 2nd Ed. San Diego, CA: Academic Press, 2002: 1361–1385

[5] Sahni M, Guenther HL, Fleisch H, Collin P, Martin TJ. Bisphosphonates act on rat bone resorption through the mediation of osteoblasts. J Clin Invest 1993; 91: 2004–2011

[6] Nishikawa M, Akatsu T, Katayama Y, Yasutomo Y, Kado S, Kugai N, Yamamoto M, Hagata N. Bisphosphonates act on osteoblastic cells and inhibit osteoclast formation in mouse marrow cultures. Bone 1995; 18: 9–14

[7] Vitte C, Fleisch H, Guenther HL. Bisphosphonates induce osteoblasts to secrete an inhibitor of osteoclast-mediated resorption. Endocrinology 1996; 137: 2324–2333

[8] Tokuda H, Kozawa O, Harada A, Uematsu T. Minodronate inhibits interleukin-6 synthesis in osteoblasts: Inhibition of phospholipase D activation in MC3T3-E1 cells. J Cell Biochem 1998; 69: 252–259

[9] Plotkin LI, Weinstein RS, Parfitt AM, Roberson PK, Manolagas SC, Bellido T. Prevention of osteocyte and osteoblast apoptosis by bisphosphonates and calcitonin. J Clin Invest 1999; 104: 1363–1374

[10] Reinholz GG, Getz B, Pederson L, Sanders ES, Subramaniam M, Ingle JN, Spelsberg TC. Bisphosphonates directly regulate cell proliferation, differentiation, and gene expression in human osteoblasts. Cancer Res 2000; 60: 6001–6007

[11] Viereck V, Emos G, Lauck V, Frosch KH, Blaschke S, Grundker C, Hofbauer LC. Bisphosphonates pamidronate and zoledronic acid stimulate osteoprotegerin production by primary human osteoblasts. Biochem Biophys Res Commun 2002; 291: 680–686

[12] Mackie PS, Fisher JL, Zhou H, Choong PF. Bisphosphonates regulate cell growth and gene expression in the UMR 106–01 clonal rat osteosarcoma cell line. Br J Cancer 2001; 84: 951–958

[13] Pan B, To LB, Farrugia AN, Findlay DM, Green J, Gronthos S, Evdokiou A, Lynch K, Atkins GJ, Zannettino ACW. The nitrogen-containing bisphosphonate, zoledronic acid, increases mineralization of human bone-derived cells in vitro. Bone 2004; 34: 112–123

[14] Pan B, Farrugia AN, To LB, Findlay DM, Green J, Lynch K, Zannettino ACW. The nitrogen-containing bisphosphonate, zoledronic acid, influences RANKL expression in human osteoblast-like cells by activating TNF-α converting enzyme (TACE). J Bone Miner Res 2004; 19: 147–154

[15] Ferrara N, Davis-Smyth T. The biology of vascular endothelial growth factor. Endocrine Rev 1997; 18: 4–25

[16] Gerber HP, Vu TH, Ryan AM, Kowalski J, Werb Z, Ferrara N. VEGF couples hypertrophic cartilage remodeling, ossification and angiogenesis during endochondral bone formation. Nat Med 1999; 5: 623–662

[17] Harada S, Thomas KA. Vascular endothelial growth factors. In: Bilezikian JP, Ratsz LG, Rodan GA (eds). Principles of Bone Biology 2nd Ed. San Diego, CA: Academic Press, 2002: 883–902

[18] Miwa M, Tokuda H, Tsushita K, Kotoyori J, Takahashi Y, Ozaki N, Kozawa O, Oiso Y. Involvement of pertussis toxin-sensitive GTP-binding protein in prostaglandin $F_{2\alpha}$-induced phosphoinositide hydrolysis in

osteoblast-like cells. Biochem Biophys Res Commun 1990; 171: 1229–1235
[19] Kozawa O, Suzuki A, Kotoyori J, Tokuda H, Watanabe Y, Ito Y, Oiso Y. 1994 Prostaglandin $F_{2\alpha}$ activates phospholipase D independently from activation of protein kinase C in osteoblast-like cells. J Cell Biochem 1994; 55: 373–379
[20] Nishizuka Y. Intracellular signaling by hydrolysis of phospholipids and activation of protein kinase C. Science 1992; 258: 607–614
[21] Exton JH. Regulation of phospholipase D. Biochim Biophys Acta 1999; 1439: 121–133
[22] Tokuda H, Harada A, Hirade K, Matsuno H, Ito H, Kato K, Oiso Y, Kozawa O. Incadronate amplifies prostaglandin $F_{2\alpha}$-induced vascular endothelial growth factor synthesis in osteoblasts. Enhancement of MAPK activity. J Biol Chem 2003; 278: 18930–18937
[23] Yoshida M, Tokuda H, Ishisaki A, Kanno Y, Harada A, Shimuzu K, Kozawa O. Tiludronate inhibits prostaglandin $F_{2\alpha}$-induced vascular endothelial growth factor synthesis in osteoblasts. Mol Cell Endocrinol 2005; 236: 59–66
[24] Sudo M, Kodama H, Amagai Y, Yamamoto S, Kasai S. In vitro differentiation and calcification in a new clonal osteogenic cell line derived from newborn mouse calvaria. J Cell Biol 1983; 96: 191–198
[25] Kanno Y, Ishisaki A, Yoshida M, Nakajima K, Tokuda H, Numata O, Kozawa O. Adenylyl cyclase-cAMP system inhibits thyroid hormone-stimulated osteocalcin synthesis in osteoblasts. Mol Cell Endocrinol 2005; 229: 75–82
[26] Noda T, Tokuda H, Yoshida M, Yasuda E, Hanai Y, Takai S, Kozawa O. Possible involvement of phosphatidylinositol 3-kinase/Akt pathway in insulin-like growth factor-I-induced alkaline phosphatase activity in osteoblasts. Horm Metab Res 2005; 37: 270–274
[27] Kozawa O, Suzuki A, Tokuda H, Uematsu T. Prostaglandin $F_{2\alpha}$ stimulates interleukin-6 synthesis via activation of PKC in osteoblast-like cells. Am J Physiol 1997; 272: E208–E211
[28] Laemmli UK. Cleavage of structural proteins during the assembly of the head of bacteriophage T4. Nature 1970; 227: 680–685
[29] Kato K, Ito K., Hasegawa K, Inaguma Y, Kozawa O, Asano T. Modulation of the stress-induced synthesis of hsp27 and αB-crystalin by cyclic AMP in C6 rat glioma cells. J Neurochem 1996; 66: 946–950
[30] Nishizuka Y. Studies and perspectives of protein kinase C. Science 1986; 233: 305–312
[31] Hatakeyama D, Kozawa O, Otsuka T, Shibata T, Uematsu T. Zinc suppresses IL-6 synthesis by prostaglandin F2α in osteoblasts: inhibition of phospholipase C and phospholipase D. J Cell Biochem 2002; 85: 621–628
[32] Widmann C, Gibson S, Jarpe MB, Johnson GL. Mitogen-activated protein kinase: conservation of a three-kinase module from yeast to human. Physiol Rev 1999; 79: 143–180
[33] Marx RE. Pamidronate (Aredia) and zoledronate (Zometa) induced avascular necrosis of the jaws: a growing epidemic. J Oral Maxillofac Surg 2003; 61: 1115–1118
[34] Carter GD, Goss AN. Bisphosphonates and avascular necrosis of the jaws. Aust Dent J 2003; 48: 268
[35] Tokuda H, Kozawa O, Harada A, Uematsu T. p42/p44 mitogen-activated protein kinase activation is involved in prostaglandin $F_{2\alpha}$-induced interleukin-6 synthesis in osteoblasts. Cell Signal 1999; 11: 325–330

Journal of Cellular Biochemistry 98:1249–1256 (2006)

Phosphatidylinositol 3-Kinase/Akt Plays a Role in Sphingosine 1-Phosphate-Stimulated HSP27 Induction in Osteoblasts

Shinji Takai,[1] Haruhiko Tokuda,[1,2] Rie Matsushima-Nishiwaki,[1] Yoshiteru Hanai,[1,2] Kanefusa Kato,[3] and Osamu Kozawa[1]*

[1]Department of Pharmacology, Gifu University Graduate School of Medicine, Gifu 501-1194, Japan
[2]Department of Clinical Laboratory, National Hospital for Geriatric Medicine, National Center for Geriatrics and Gerontology, Obu, Aichi 474-8511, Japan
[3]Department of Biochemistry, Institute for Developmental Research, Aichi Human Service Center, Kasugai 486-0392, Japan

Abstract We previously reported that p38 mitogen-activated protein (MAP) kinase plays a part in sphingosine 1-phosphate-stimulated heat shock protein 27 (HSP27) induction in osteoblast-like MC3T3-E1 cells. In the present study, we investigated whether phosphatidylinositol 3-kinase (PI3K)/protein kinase B (Akt) is involved in the induction of HSP27 in these cells. Sphingosine 1-phosphate time dependently induced the phosphorylation of Akt. Akt inhibitor, 1L-6-hydroxymethyl-*chiro*-inositol 2-(*R*)-2-*O*-methyl-3-*O*-octadecylcarbonate, reduced the HSP27 induction stimulated by sphingosine 1-phosphate. The sphingosine 1-phosphate-induced phosphorylation of GSK-3β was suppressed by Akt inhibitor. The sphingosine 1-phosphate-induced HSP27 levels were attenuated by LY294002 or wortmannin, PI3K inhibitors. Furthermore, LY294002 or Akt inhibitor did not affect the sphingosine 1-phosphate-induced phosphorylation of p38 MAP kinase and SB203580, a p38 MAP kinase inhibitor, had little effect on the phosphorylation of Akt. These results suggest that PI3K/Akt plays a part in the sphingosine 1-phosphate-stimulated induction of HSP27, maybe independently of p38 MAP kinase, in osteoblasts. J. Cell. Biochem. 98: 1249–1256, 2006.

Key words: sphingosine 1-phosphate; heat shock protein; protein kinase; osteoblast

Sphingosine 1-phosphate is a metabolite of sphingomyelin. It is generally recognized that sphingomyelin is catalyzed by sphingomyelinase, resulting in the formation of ceramide, which is subsequently metabolized to sphingosine and sphingosine 1-phosphate [Spiegel and Merrill, 1996]. Accumulating evidence indicates that sphingosine 1-phosphate plays an important role in essential cellular functions such as proliferation, differentiation, and migration [Spiegel and Merrill, 1996; Spiegel and Milstein, 2003; Sanchez and Hla, 2004]. Bone metabolism is regulated by two functional cells, osteoblasts and osteoclasts, responsible for bone formation and bone resorption, respectively [Nijweide et al., 1986]. As for osteoblasts, it has been reported that sphingosine 1-phosphate prevents apoptosis via phosphatidylinositol 3-kinase (PI3K) in primary calvaria rat osteoblasts and human osteosarcoma SaOS-2 cells [Grey et al., 2002]. In our study [Kozawa et al., 1997a], we have previously reported that sphingosine 1-phosphate stimulates interleukin-6 synthesis in osteoblast-like MC3T3-E1 cells. However, the exact mechanism of sphingosine 1-phosphate in bone metabolism has not yet been precisely clarified.

Heat shock proteins (HSP) are expressed in both prokaryotic and eukaryotic cells in response to the biological stress such as heat stress and chemical stress [Hendrick and Hartl, 1993]. HSPs are classified into high-molecular-weight

Grant sponsor: Ministry of Education, Science, Sports and Culture of Japan; Grant numbers: 16590873, 16591482; Grant sponsor: Ministry of Health, Labour and Welfare of Japan; Grant numbers: 15A-1, 15C-2.

*Correspondence to: Osamu Kozawa, Department of Pharmacology, Gifu University Graduate School of Medicine, Gifu 501-1194, Japan. E-mail: okozawa@cc.gifu-u.ac.jp

Received 7 November 2005; Accepted 29 December 2005
DOI 10.1002/jcb.20846
Published online 2 March 2006 in Wiley InterScience (www.interscience.wiley.com).

HSPs and low-molecular-weight HSPs based on apparent molecular sizes. Low-molecular-weight HSPs with molecular masses from 10 to 30 kDa, such as HSP27 and αB-crystallin have high homology in amino acid sequences [Inaguma et al., 1993; Benjamin and McMillan, 1998]. Though the functions of the low-molecular-weight HSPs are known less than those of the high-molecular-weight HSPs, it is generally accepted that they may have chaperoning functions like the high-molecular-weight HSPs [Inaguma et al., 1993; Benjamin and McMillan, 1998]. HSP27 becomes rapidly phosphorylated in response to various stresses, as well as to exposure to cyotokines and mitogens [Gaestel et al., 1991; Landry et al., 1992]. Under unstimulated conditions, HSP27 exists as a high-molecular weight aggregated form. It is rapidly dissociated as a result of phosphorylation [Kato et al., 1994; Rogalla et al., 1999]. The phosphorylation-induced dissociation from the aggregated form correlates with the loss of molecular chaperone activity [Kato et al., 1994; Rogalla et al., 1999]. In a previous study [Kozawa et al., 1999], we have shown that sphingosine 1-phosphate stimulates the induction of HSP27 in osteoblast-like MC3T3-E1 cells and that p38 mitogen-activated protein (MAP) kinase is involved in the HSP27 induction.

It is well known that Akt, also called protein kinase B, is a serine/threonine protein kinase that plays crucial roles in mediating intracellular signaling of variety of agonists including insulin-like growth factor-I, platelet-derived growth factor (PDGF), and cytokines [Downward, 1995; Franke et al., 1995; Coffer et al., 1998]. It has been shown that Akt regulates biological functions such as gene expression, survival, and oncogenesis [Coffer et al., 1998]. Accumulating evidence suggests that PI3K functions at an upstream from Akt [Chan et al., 1999; Cantley, 2002]. Akt containing a pleckstrin homology domain is recruited to the plasma membrane by the lipid product of PI3K and activated. As for osteoblasts, it has been reported that IGF-I and PDGF induce translocation of Akt to the nucleus [Borgatti et al., 2000]. In addition, recently, Akt is reportedly activated by cyclic stretch or androgen [Danciu et al., 2003; Kang et al., 2004]. We have recently shown that Akt plays an important role in insulin-like growth factor-I-stimulated alkaline phosphatase activity in MC3T3-E1 cells [Noda et al., 2005]. However, the correlation between HSP27 and PI3K/Akt in osteoblasts has not yet been clarified.

In the present study, we investigated whether PI3K/Akt is involved in sphingosine 1-phosphate-stimulated phosphorylation of HSP27 in osteoblast-like MC3T3-E1 cells. We here show that PI3K/Akt pathway is involved in the sphingosine 1-phosphate-stimulated induction of HSP27, maybe independently of p38 MAP kinase, in these cells.

MATERIALS AND METHODS

Materials

Sphingosine 1-phosphate and β-actin antibodies were purchased from Sigma Chemical Co. (St. Louis, MO). Akt inhibitor (1L-6-hydroxymethyl-*chiro*-inositol 2-(*R*)-2-*O*-methyl-3-*O*-octadecylcarbonate), LY294002, wortmannin, and SB203580 were obtained from Calbiochem-Novabiochem (La Jolla, CA). Phospho-specific Akt antibodies, Akt antibodies, phospho-specific p38 MAP kinase antibodies, p38 MAP kinase antibodies, phospho-specific GSK-3β antibodies, and GSK-3β antibodies were purchased from Cell Signaling Technology, Inc. (Beverly, MA). HSP27 antibodies were obtained from R&D Systems, Inc. (Minneapolis, MN). An ECL Western blotting detection system was obtained from Amersham Japan (Tokyo, Japan). Other materials and chemicals were obtained from commercial sources. Sphingosine 1-phosphate, Akt inhibitor LY294002, wortmannin, and SB203580 were dissolved in dimethyl sulfoxide (DMSO). All inhibitors became soluble in the cell culture media after once dissolved in DMSO. The maximum concentration of DMSO was 0.1%, which did not affect Western blot analysis.

Cell Culture

Cloned osteoblast-like MC3T3-E1 cells derived from newborn mouse calvaria [Sudo et al., 1983] were maintained as previously described [Kozawa et al., 1997b]. Briefly, the cells were cultured in α-minimum essential medium (α-MEM) containing 10% fetal calf serum (FCS) at 37°C in a humidified atmosphere of 5% CO_2/95% air. The cells were seeded into 90-mm diameter dishes (25×10^4/dish) in α-MEM containing 10% FCS. After 5 days, the medium was exchanged for α-MEM containing 0.3% FCS. The cells were used for experiments after 48 h. When indicated, the cells were pretreated with Akt

inhibitor, wortmannin, LY294002, or SB203580 for 60 min prior to stimulation of sphingosine 1-phosphate.

Western Blot Analysis

Cultured cells were stimulated by sphingosine 1-phosphate in serum-free α-MEM for the indicated periods. Cells were washed twice with phosphate-buffered saline and then lysed, homogenized, sonicated, and immediately boiled in a lysis buffer containing 62.5 mM Tris/Cl, pH 6.8, 2% sodium dodecyl sulfate (SDS), 50 mM dithiothreitol, and 10% glycerol. The sample was used for the analysis by Western blotting. SDS–polyacrylamide gel electrophoresis (PAGE) was performed by the method of Laemmli [Laemmli, 1970] in 10% polyacrylamide gel. Western blot analysis was performed as described previously [Kato et al., 1996], using phospho-specific Akt antibodies, Akt antibodies, HSP27 antibodies, phospho-specific p38 MAP kinase antibodies, p38 MAP kinase antibodies, phospho-specific GSK-3β antibodies, or GSK-3β antibodies with peroxidase-labeled antibodies raised in goat against rabbit IgG being used as second antibodies. Peroxidase activity on PVDF membranes was visualized on X-ray film by means of the ECL Western blotting detection system and was quantitated using NIH image software. All of Western blot analyses were repeated at least three times in independent experiments.

Statistical Analysis

The data were analyzed by ANOVA followed by Bonferroni method for multiple comparisons between pairs, and a $P<0.05$ was considered significant. All data are presented as the mean ± SD of triplicate determinations.

RESULTS

Time-Dependent Effects of Sphingosine 1-Phosphate on the Phosphorylation of Akt in MC3T3-E1 Cells

Sphingosine 1-phosphate significantly stimulates the phosphorylation of Akt in osteoblast-like MC3T3-E1 cells in a time-dependent manner (Fig. 1). The phosphorylation of Akt was markedly observed at 5 min after the sphingosine 1-phosphate-stimulation. The phosphorylation reached its peak at 15 min after the stimulation and decreased thereafter.

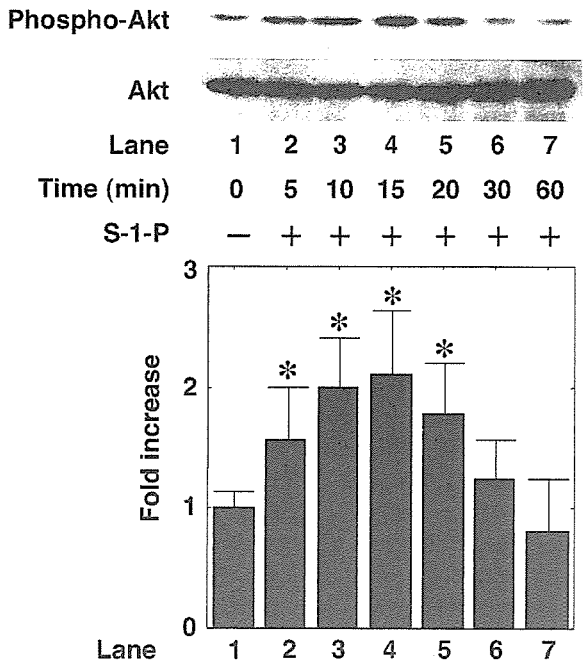

Fig. 1. Effect of sphingosine 1-phosphate (S-1-P) on the phosphorylation of Akt in MC3T3-E1 cells. The cultured cells were stimulated with 30 μM S-1-P for the indicated periods. The extracts of cells were subjected to SDS–PAGE with subsequent Western blotting analysis with antibodies against phospho-specific Akt or Akt. The histogram shows quantitative representations of the levels of S-1-P-induced phosphorylation obtained from laser densitometric analysis of three independent experiments. Similar results were obtained with two additional and different cell preparations. Each value represents the mean ± SD of triplicate determinations from triplicate independent cell preparations. *$P< 0.05$, compared to the value of control.

Effect of Akt Inhibitor on the Induction of HSP27 in MC3T3-E1 Cells

Then we examined the effect of Akt inhibitor (1L-6-hydroxymethyl-*chiro*-inositol 2-(*R*)-2-*O*-methyl-3-*O*-octadecylcarbonate) [Hu et al., 2000] on the sphingosine 1-phosphate-stimulated induction of HSP27. Akt inhibitor partially suppressed the sphingosine 1-phosphate-induced up-regulation of HSP27 levels (Fig. 2). Akt inhibitor (50 μM) caused about 40% reduction in the sphingosine 1-phosphate-effect.

We have previously shown that sphingosine 1-phosphate stimulates HSP27 induction at least in part via p38 MAP kinase in osteoblasts [Kozawa et al., 1999]. However, Akt inhibitor did not influence the sphingosine 1-phosphate-induced phosphorylation of p38 MAP kinase in MC3T3-E1 cells (data not shown). It is well known that GSK-3β is one of

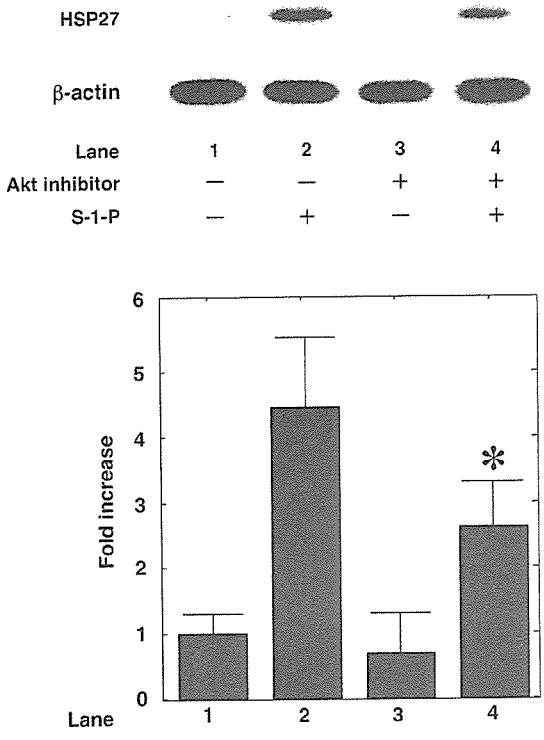

Fig. 2. Effect of Akt inhibitor on the sphingosine 1-phosphate (S-1-P)-induced levels of HSP27 in MC3T3-E1 cells. The cultured cells were pretreated with 50 μM Akt inhibitor for 60 min, and then stimulated by 30 μM of S-1-P or vehicle for 6 h. The extracts of cells were subjected to SDS–PAGE with subsequent Western blotting analysis with antibodies against HSP27 or β-actin. The histogram shows quantitative representations of the levels of S-1-P-induced HSP27 after normalization to levels of β-actin. Similar results were obtained with two additional and different cell preparations. Each value represents the mean ± SD of triplicate determinations from triplicate independent cell preparations. *$P < 0.05$, compared to the value of S-1-P.

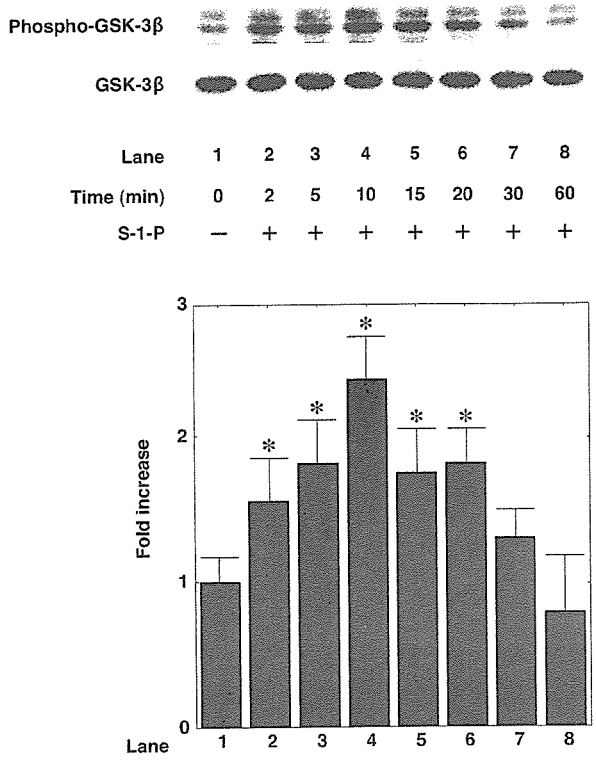

Fig. 3. Effect of sphingosine 1-phosphate (S-1-P) on the phosphorylation of GSK-3β in MC3T3-E1 cells. The cultured cells were stimulated with 30 μM S-1-P for the indicated periods. The extracts of cells were subjected to SDS–PAGE with subsequent Western blotting analysis with antibodies against phospho-specific GSK-3β or GSK-3β. The histogram shows quantitative representations of the levels of S-1-P-induced phosphorylation obtained from laser densitometric analysis of three independent experiments. Similar results were obtained with two additional and different cell preparations. Each value represents the mean ± SD of triplicate determinations from triplicate independent cell preparations. *$P < 0.05$, compared to the value of control.

the Akt substrates [Cross et al., 1995]. We found that GSK-3β was time dependently phosphorylated by sphingosine 1-phosphate (Fig. 3). In addition, Akt inhibitor attenuated the sphingosine 1-phosphate-induced phosphorylation of GSK-3β, suggesting that the Akt-mediating pathway actually functions in sphingosine 1-phosphate-stimulated MC3T3-E1 cells (Fig. 4). Akt inhibitor (50 μM) caused about 50% reduction in the sphingosine 1-phosphate-effect.

Effects of LY294002 and Wortmannin on the Sphingosine 1-Phosphate-Induced Phosphorylation of Akt in MC3T3-E1 Cells

In order to clarify whether PI3K acts at a point upstream from Akt, we examined the effect of LY294002, a specific inhibitor of PI3K [Vlahos et al., 1994], on the sphingosine 1-phosphate-induced phosphorylation of Akt. LY294002 dose dependently suppressed the sphingosine 1-phosphate-induced Akt phosphorylation (Fig. 5A). LY294002 (10 μM) caused almost complete reduction in the sphingosine 1-phosphate-effect. Wortmannin, another PI3K inhibitor [Arcaro and Wymann, 1993], also suppressed the phosphorylation of Akt (Fig. 5B). Wortmannin (10 μM) caused about 40% reduction in the sphingosine 1-phosphate-effect. However, LY294002 did not affect the sphingosine 1-phosphate-induced phosphorylation of p38 MAP kinase in MC3T3-E1 cells (data not shown). In addition, SB203580, a specific inhibitor of p38 MAP kinase [Cuenda et al., 1995] failed to affect the sphingosine 1-phosphate-induced phosphorylation of Akt (data not shown).

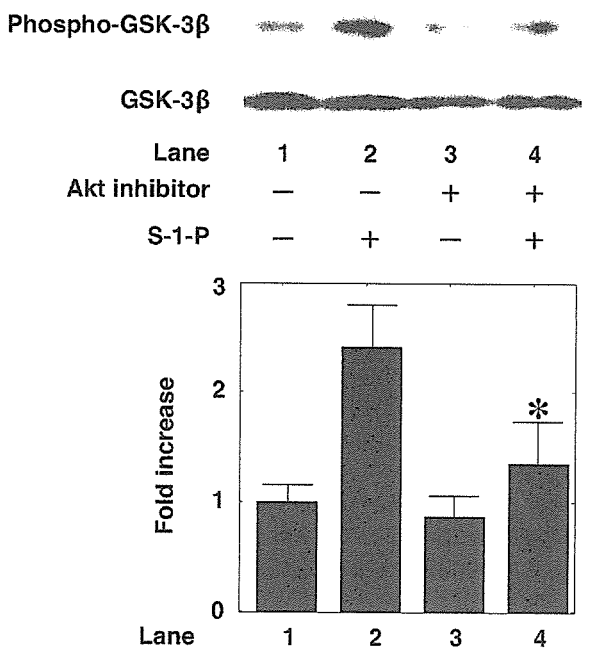

Fig. 4. Effect of Akt inhibitor on the sphingosine 1-phosphate (S-1-P)-induced phosphorylation of GSK-3β in MC3T3-E1 cells. The cultured cells were pretreated with 50 μM Akt inhibitor for 60 min, and then stimulated by 30 μM S-1-P or vehicle for 20 min. The extracts of cells were subjected to SDS–PAGE with subsequent Western blotting analysis with antibodies against phospho-specific GSK-3β or GSK-3β. The histogram shows quantitative representations of the levels of S-1-P-induced phosphorylation obtained from laser densitometric analysis of three independent experiments. Similar results were obtained with two additional and different cell preparations. Each value represents the mean ± SD of triplicate determinations from triplicate independent cell preparations. $*P < 0.05$, compared to the value of S-1-P.

Effects of LY294002 and Wortmannin on the Sphingosine 1-Phosphate-Stimulated Induction of HSP27 in MC3T3-E1 Cells

LY294002 significantly suppressed the sphingosine 1-phosphate-stimulated induction of HSP27 in a dose dependent manner between

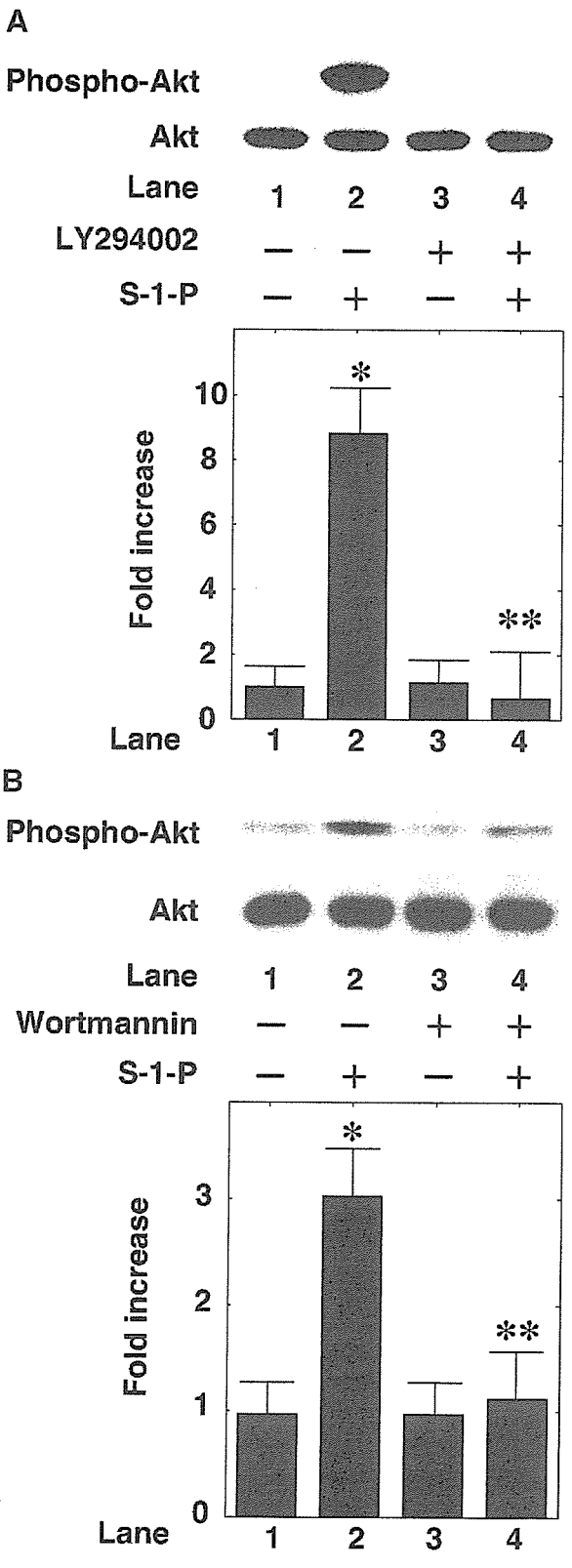

Fig. 5. Effects of LY294002 or wortmannin on the sphingosine 1-phosphate (S-1-P)-induced phosphorylation of Akt in MC3T3-E1 cells. The cultured cells were pretreated with 10 μM LY294002 (**A**) or 10 μM wortmannin (**B**) for 60 min, and then stimulated by 30 μM S-1-P or vehicle for 20 min. The extracts of cells were subjected to SDS–PAGE with subsequent Western blotting analysis with antibodies against phospho-specific Akt or Akt. The histogram shows quantitative representations of the levels of S-1-P-induced phosphorylation obtained from laser densitometric analysis of three independent experiments. Similar results were obtained with two additional and different cell preparations. Each value represents the mean ± SD of triplicate determinations from triplicate independent cell preparations. $*P < 0.05$, compared to the value of control (without agonist and inhibitor). $**P < 0.05$, compared to the value of S-1-P alone.

10 and 50 μM (Fig. 6A). Additionally, wortmannin markedly reduced the induction of HSP27 similarly to LY294002 (Fig. 6B).

DISCUSSION

We have previously shown that sphingosine 1-phosphate stimulates induction of HSP27 in osteoblast-like MC3T3-E1 cells and that p38 MAP kinase takes a part in the sphingosine 1-phosphate-effect [Kozawa et al., 1999]. In the present study, we first demonstrated that sphingosine 1-phosphate stimulated the phosphorylation of Akt in a time-dependent manner in MC3T3-E1 cells. In addition, we showed that PI3K inhibitors such as LY294002 and wortmannin, suppressed the sphingosine 1-phopshate-induced phosphorylation of Akt, suggesting that Akt functions at a point downstream from PI3K in these cells. PI3K is recruited upon growth factor receptor activation and produces 3′ phosphoinositide lipids [Dudek et al., 1997; Katso et al., 2001]. The lipid products of PI3K act as second messengers by binding to and activating diverse cellular target proteins. These events constitute the start of a complex signaling cascade, which ultimately results in the mediation of cellular activities such as proliferation, differentiation, chemotaxis, and survival. The PI3K/Akt signaling pathway is currently considered to play a critical role in mediating survival signals in a wide range of cell types. The recent identification of a number of substrates for the serine/threonine kinase Akt suggests that it blocks cell death by both impinging on the cytoplasmic cell death machinery and by regulating the expression of genes involved in cell death and survival. In addition, recent experiments suggest that Akt may also use metabolic pathways to regulate cell survival [Brunet et al., 2001; Masuyama et al., 2001].

Therefore, we next examined the correlation between the sphingosine 1-phosphate-stimulated induction of HSP27 and PI3K/Akt in osteoblast-like MC3T3-E1 cells. In the present study, the sphingosine 1-phosphate-stimulated HSP27 induction was reduced by Akt inhibitor. As for Akt inhibitor, 1L-6-hydroxymethyl-*chiro*-inositol 2-(*R*)-2-*O*-methyl-3-*O*-octadecylcarbonate [Hu et al., 2000], we found that it blocked the phosphorylation of GSK-3β, one of the Akt substrates [Cross et al., 1995]. In addition, we showed that PI3K inhibitors also suppressed

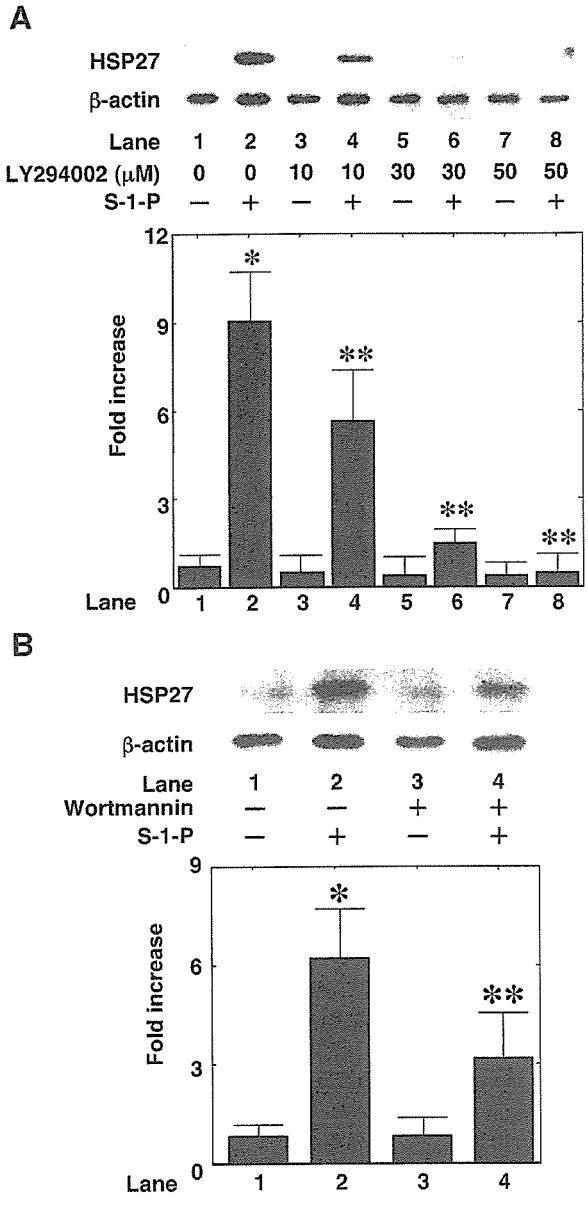

Fig. 6. Effects of LY294002 or wortmannin on the sphingosine 1-phosphate (S-1-P)-induced levels of HSP27 in MC3T3-E1 cells. The cultured cells were pretreated with various doses of LY294002 (**A**) or 50 μM wortmannin (**B**) for 60 min, and then stimulated by 30 μM S-1-P or vehicle for 6 h. The extracts of cells were subjected to SDS–PAGE with subsequent Western blotting analysis with antibodies against HSP27 or β-actin. The histogram shows quantitative representations of the levels of S-1-P-induced HSP27 after normalization to levels of β-actin. Similar results were obtained with two additional and different cell preparations. Each value represents the mean ± SD of triplicate determinations from triplicate independent cell preparations. $^{*}P < 0.05$, compared to the value of control. $^{**}P < 0.05$, compared to the value of S-1-P alone.

the sphingosine 1-phosphate-stimulated HSP27 induction thorough the reduction of the sphingosine 1-phosphate-induced Akt phosphorylation. Therefore, based on our findings, it is most likely that the sphingosine 1-phosphate-stimulated induction of HSP27 is regulated by PI3K/Akt in osteoblast-like MC3T3-E1 cells.

We have previously reported that the activation of p38 MAP kinase is involved in HSP27 induction by sphingosine 1-phosphate in osteoblast-like MC3T3-E1 cells [Kozawa et al., 1999]. Therefore, we investigated to clarify the relationship between p38 MAP kinase and PI3K/Akt in these cells. Akt inhibitor and PI3K inhibitor, LY294002 [Vlahos et al., 1994], failed to influence the sphingosine 1-phosphate-induced phosphorylation of p38 MAP kinase in MC3T3-E1 cells, and p38 MAP kinase inhibitor, SB203580 [Cuenda et al., 1995], had little effect on the sphingosine 1-phosphate-induced phosphorylation of Akt. In addition, the inhibitory effect of Akt inhibitor or wortmannin on the sphingosine 1-phosphate-stimulated HSP27 induction was partial. We have previously shown that the suppressive effect of SB203580 on the HSP27 induction was partial [Kozawa et al., 1999]. These findings suggest that PI3K/Akt pathway plays a role at least in part in addition to p38 MAP kinase pathway in the sphingosine 1-phosphate-stimulated HSP27 induction in MC3T3-E1 cells. Taking these results into account as a whole, it is most likely that sphingosine 1-phosphate stimulates the induction of HSP27 probably via two independent pathways, PI3K/Akt and p38 MAP kinase, in osteoblast-like MC3T3-E1 cells.

It is recognized that HSP27 is present at two forms, an aggregated form and a dissociated small form in unstressed conditions [Benjamin and McMillan, 1998]. It has been shown that HSP27 is constitutively expressed at high levels in various tissues and cells, especially in skeletal muscle cells and smooth muscle cells [Benjamin and McMillan, 1998]. Post-translational modifications such as phosphorylation and oligomerization are crucial regulators of its functions [Benjamin and McMillan, 1998]. In our previous study [Kato et al., 1994], we have reported that HSP27 is dissociated concomitantly with the phosphorylation of the aggregated form of HSP27. In addition, we have shown that conversion from the non-phosphorylated, aggregated form of HSP27 to the phosphorylated, dissociated form results in decreased tolerance to heat stress [Kato et al., 1994]. It has been shown that estrogen-induced resistance to osteoblast apoptosis is associated with increased HSP27 expression [Cooper et al., 2000]. We speculate that expression of HSP27 via p38 MAP kinase and PI3K/Akt in osteoblasts might be related to the maintenance of the number of viable osteoblasts in bone tissue. Interestingly, sphingosine 1-phosphate reportedly prevents apoptosis in primary rat osteoblasts and human osteosarcoma SaOS-2 cells [Grey et al., 2002]. Taking our findings into account, it is probable that sphingosine 1-phosphate directly affects osteoblasts through the induction of HSP27 through PI3K/Akt and p38 MAP kinase. However, the physiological significance of HSP27 in osteoblasts has not yet been precisely clarified. Further investigations are necessary to clarify the exact roles of HSP27 in osteoblasts.

In conclusion, these results strongly suggest that sphingosine 1-phosphate stimulates the induction of HSP27 via PI3K/Akt pathway in addition to p38 MAP kinase in osteoblasts.

ACKNOWLEDGMENTS

This work was supported in part by Grant-in-Aid for Scientific Research (16590873 and 16591482) for the Ministry of Education, Science, Sports and Culture of Japan, the Research Grants for Longevity Sciences (15A-1 and 15C-2), Research on Proteomics and Research on Fracture and Dimentia from Ministry of Health, Labour and Welfare of Japan.

REFERENCES

Arcaro A, Wymann MP. 1993. Wortmannin is a potent phosphatidylinositol 3-kinase inhibitor: The role of phosphatidylinositol 3,4,5-trisphosphate in neutrophil responses. Biochem J 296:297–301.

Benjamin IJ, McMillan DR. 1998. Stress (heat shock) proteins: Molecular chaperones in cardiovascular biology and disease. Circ Res 83:117–132.

Borgatti P, Martelli AM, Bellacosa A, Casto R, Massari L, Capitani S, Neri LM. 2000. Translocation of Akt/PKB to the nucleus of osteoblast-like MC3T3-E1 cells exposed to proliferative growth factors. FEBS Lett 477:27–32.

Brunet A, Datta SR, Greenberg ME. 2001. Transcription-dependent and -independent control of neuronal survival by the PI3K-Akt signaling pathway. Curr Opin Neurobiol 11:297–305.

Cantley LC. 2002. The phosphoinositide 3-kinase pathway. Science 296:1655–1657.

Chan TO, Rittenhouse SE, Tsichlis PN. 1999. AKT/PKB and other D3 phosphoinositide-regulated kinases: Kinase activation by phosphoinositide-dependent phosphorylation. Annu Rev Biochem 68:965–1014.

Coffer PJ, Jin J, Woodgett JR. 1998. Protein kinase B (c-Akt): A multifunctional mediator of phosphatidylinositol 3-kinase activation. Biochem J 335:1–13.

Cooper LF, Tiffee JC, Griffin JP, Hamano H, Guo Z. 2000. Estrogen-induced resistance to osteoblast apoptosis is associated with increased hsp27 expression. J Cell Physiol 185:401–407.

Cross DA, Alessi DR, Cohen P, Andjelkovich M, Hemmings BA. 1995. Inhibition of glycogen synthase kinase-3 by insulin mediated by protein kinase B. Nature 378:785–789.

Cuenda A, Rouse J, Doza YN, Meier R, Cohen P, Gallagher TF, Young PR, Lee JC. 1995. SB203580 is a specific inhibitor of a MAP kinase homologue which is stimulated by cellular stresses and interleukin-1. FEBS Lett 364: 229–233.

Danciu TE, Adam RM, Naruse K, Freeman MR, Hauschka PV. 2003. Calcium regulates the PI3K-Akt pathway in stretched osteoblasts. FEBS Lett 536:193–197.

Downward J. 1995. Signal transduction. A target for PI(3) kinase. Nature 376:553–554.

Dudek H, Datta SR, Franke TF, Birnbaum MJ, Yao R, Cooper GM, Segal RA, Kaplan DR, Greenberg ME. 1997. Regulation of neuronal survival by the serine-threonine protein kinase Akt. Science 275:661–665.

Franke TF, Yang SI, Chan TO, Datta K, Kazlauskas A, Morrison DK, Kaplan DR, Tsichlis PN. 1995. The protein kinase encoded by the Akt proto-oncogene is a target of the PDGF-activated phosphatidylinositol 3-kinase. Cell 81:727–736.

Gaestel M, Schroder W, Benndorf R, Lippmann C, Buchner K, Hucho F, Erdmann VA, Bielka H. 1991. Identification of the phosphorylation sites of the murine small heat shock protein hsp25. J Biol Chem 266:14721–14724.

Grey A, Chen Q, Callon K, Xu X, Reid IR, Cornish J. 2002. The phospholipids sphingosine 1-phosphate and lysophosphatidic acid prevent apoptosis in osteoblastic cells via a signaling pathway involving Gi proteins and phosphatidylinositol-3 kinase. Endocrinology 143:4755–4763.

Hendrick JP, Hartl FU. 1993. Molecular chaperone functions of heat-shock proteins. Annu Rev Biochem 62:349–384.

Hu Y, Qiao L, Wang S, Rong SB, Meuillet EJ, Berggren M, Gallegos A, Powis G, Kozikowski AP. 2000. 3-(Hydroxymethyl)-bearing phosphatidylinositol ether lipid analogues and carbonate surrogates block PI3-K, Akt, and cancer cell growth. J Med Chem 43:3045–3051.

Inaguma Y, Goto S, Shinohara H, Hasegawa K, Ohshima K, Kato K. 1993. Physiological and pathological changes in levels of the two small stress proteins, HSP27 and alpha B crystallin, in rat hindlimb muscles. J Biochem (Tokyo) 114:378–384.

Kang HY, Cho CL, Huang KL, Wang JC, Hu YC, Lin HK, Chang C, Huang KE. 2004. Nongenomic androgen activation of phosphatidylinositol 3-kinase/Akt signaling pathway in MC3T3-E1 osteoblasts. J Bone Miner Res 19: 1181–1190.

Kato K, Hasegawa K, Goto S, Inaguma Y. 1994. Dissociation as a result of phosphorylation of an aggregated form of the small stress protein, hsp27. J Biol Chem 269:11274–11278.

Kato K, Ito H, Hasegawa K, Inaguma Y, Kozawa O, Asano T. 1996. Modulation of the stress-induced synthesis of hsp27 and alpha B-crystallin by cyclic AMP in C6 rat glioma cells. J Neurochem 66:946–950.

Katso R, Okkenhaug K, Ahmadi K, White S, Timms J, Waterfield MD. 2001. Cellular function of phosphoinositide 3-kinases: Implications for development, homeostasis, and cancer. Annu Rev Cell Dev Biol 17:615–675.

Kozawa O, Tokuda H, Matsuno H, Uematsu T. 1997a. Activation of mitogen-activated protein kinase is involved in sphingosine 1-phosphate-stimulated interleukin-6 synthesis in osteoblasts. FEBS Lett 418:149–151.

Kozawa O, Suzuki A, Tokuda H, Uematsu T. 1997b. Prostaglandin $F_{2\alpha}$ stimulates interleukin-6 synthesis via activation of PKC in osteoblast-like cells. Am J Physiol 272:E208–E211.

Kozawa O, Niwa M, Matsuno H, Tokuda H, Miwa M, Ito H, Kato K, Uematsu T. 1999. Sphingosine 1-phosphate induces heat shock protein 27 via p38 mitogen-activated protein kinase activation in osteoblasts. J Bone Miner Res 92:1203–1211.

Laemmli UK. 1970. Cleavage of structural proteins during the assembly of the head of bacteriophage T4. Nature 227:680–685.

Landry J, Lambert H, Zhou M, Lavoie JN, Hickey E, Weber LA, Anderson CW. 1992. Human HSP27 is phosphorylated at serines 78 and 82 by heat shock and mitogen-activated kinases that recognize the same amino acid motif as S6 kinase II. J Biol Chem 267:794–803.

Masuyama N, Oishi K, Mori Y, Ueno T, Takahama Y, Gotoh Y. 2001. Akt inhibits the orphan nuclear receptor Nur77 and T-cell apoptosis. J Biol Chem 276:32799–32805.

Nijweide PJ, Burger EH, Feyen JHM. 1986. Cells of bone: Proliferation, differentiation, and hormonal regulation. Physiol Rev 86:855–886.

Noda T, Tokuda H, Yoshida M, Yasuda E, Hanai Y, Takai S, Kozawa O. 2005. Possible involvement of phosphatidylinositol 3-kinase/Akt pathway in insulin-like growth factor-I-induced alkaline phosphatase activity in osteoblasts. Horm Met Res 37:270–274.

Rogalla T, Ehrnsperger M, Preville X, Kotlyarov A, Lutsch G, Ducasse C, Paul C, Wieske M, Arrigo AP, Buchner J, Gaestel M. 1999. Regulation of Hsp27 oligomerization, chaperone function, and protective activity against oxidative stress/tumor necrosis factor α by phosphorylation. J Biol Chem 274:18947–18956.

Sanchez T, Hla T. 2004. Structural and functional characteristics of S1P receptors. J Cell Biochem 92: 913–922.

Spiegel S, Merrill JAH. 1996. Sphingolipid metabolism and cell growth regulation. FASEB J 10:1388–1397.

Spiegel S, Milstein S. 2003. Sphingosine-1-phosphate: An enigmatic signaling lipid. Nat Rev Mol Cell Biol 4:397–407.

Sudo H, Kodama H, Amagai Y, Yamamoto S, Kasai S. 1983. *In vitro* differentiation and calcification in a new clonal osteogenic cell line derived from newborn mouse calvaria. J Cell Biol 96:191–198.

Vlahos CJ, Matter WF, Hui KY, Brown RF. 1994. A specific inhibitor of phosphatidylinositol 3-kinase, 2-(4-morpholinyl)-8-phenyl-4H-1-benzopyran-4-one (LY294002). J Biol Chem 269:5241–5248.

ELSEVIER

Molecular and Cellular Endocrinology 251 (2006) 42–48

MCE
Molecular and Cellular Endocrinology

www.elsevier.com/locate/mce

Involvement of p44/p42 MAP kinase in insulin-like growth factor-I-induced alkaline phosphatase activity in osteoblast-like-MC3T3-E1 cells

Yoshiteru Hanai [a,c], Haruhiko Tokuda [a,c], Akira Ishisaki [d], Rie Matsushima-Nishiwaki [c], Norimi Nakamura [b], Minoru Yoshida [c], Shinji Takai [c], Toshiki Ohta [b], Osamu Kozawa [c,*]

[a] *Department of Clinical Laboratory, National Hospital for Geriatric Medicine, National Center for Geriatrics and Gerontology, Obu, Aichi 474-8511, Japan*
[b] *Department of Internal Medicine, National Hospital for Geriatric Medicine, National Center for Geriatrics and Gerontology, Obu, Aichi 474-8511, Japan*
[c] *Department of Pharmacology, Gifu University Graduate School of Medicine, Gifu 501-1194, Japan*
[d] *Department of Biochemistry and Molecular Biology, Graduate School of Dental Medicine, Hokkaido University, Sapporo 060-8586, Japan*

Received 26 January 2006; accepted 17 February 2006

Abstract

It has been shown that insulin-like growth factor-I (IGF-I) stimulates the activity of alkaline phosphatase, a marker of mature osteoblast phenotype, in osteoblasts. In the present study, we investigated the involvement of the mitogen-activated protein (MAP) kinase superfamily in the IGF-I-stimulated alkaline phosphatase activity in osteoblast-like MC3T3-E1 cells. IGF-I-stimulated alkaline phosphatase activity dose dependently in the range between 1 nM and 0.1 μM. IGF-I induced the phosphorylation of p44/p42 MAP kinase and p38 MAP kinase but not stress-activated protein kinase/c-*Jun* N-terminal kinase (SAPK/JNK). PD98059 and U0126, specific inhibitors of the upstream kinase that activates p44/p42 MAP kinase, significantly suppressed the IGF-I-induced alkaline phosphatase activity. On the contrary, SB203580 and PD169316, specific inhibitors of p38 MAP kinase, failed to affect the activity induced by IGF-I. Specific inhibitors for phosphatidylinositol 3-kinase (PI3K)/Akt pathway (LY294002 and wortmannin) also had no significant effect on IGF-I-induced p44/p42 MAP kinase phosphorylation. The phosphorylation of p44/p42 MAP kinase induced by IGF-I was reduced by U0126. These results strongly suggest that p44/p42 MAP kinase among the MAP kinase superfamily plays a role in the IGF-I-stimulated alkaline phosphatase activity in osteoblast-like MC3T3-E1 cells.

Keywords: IGF-I; Alkaline phosphatase; p44/p42 MAP kinase; Osteoblast

1. Introduction

It is well recognized that insulin-like growth factor-I (IGF-I) plays a crucial role in the regulation of growth and bone metabolism (Conover, 2000; Olney, 2003). IGF-I, which is mainly synthesized and secreted from liver, mediates a variety of the actions of growth hormone that is secreted from pituitary gland under the control of the hypothalamus. Accumulating evidence suggests that IGF-I is necessary for fracture healing (Trippel, 1998). Bone metabolism is regulated mainly by two functional cells, osteoblasts and osteoclasts, the former responsible for bone formation and the latter for bone resorption (Nijweide et al., 1986). As for osteoblasts, it has been reported that IGF-I stimulates the proliferation of these cells and synthesize bone matrix proteins (Conover, 2000). We have previously demonstrated that IGF-I induces DNA synthesis synergistically with protein kinase C activation in osteoblast-like MC3T3-E1 cells (Kozawa et al., 1989). In addition, IGF-I reportedly stimulates alkaline phosphatase activity, a marker of mature osteoblast phenotype (Robinson et al., 1973), in osteoblasts (Schmid et al., 1984). It is recognized that IGF-I is also produced by osteoblasts (Olney, 2003). In a previous study (Kozawa et al., 1992b), we have shown that osteoblast-like MC3T3-E1 cells secrete IGF-I resulting in inducing mineralization, and protein kinase C activation suppresses the secretion of IGF-I. Based on these findings, there is no doubt that IGF-I secreted from osteoblasts plays a pivotal role in the regulation of bone metabolism.

* Corresponding author. Tel.: +81 58 230 6214; fax: +81 58 230 6215.
E-mail address: okozawa@cc.gifu-u.ac.jp (O. Kozawa).

0303-7207/$ – see front matter © 2006 Elsevier Ireland Ltd. All rights reserved.
doi:10.1016/j.mce.2006.02.014

The mitogen-activated protein (MAP) kinase superfamily is well recognized to play crucial roles in the intracellular signaling of variety of agonists (Widmann et al., 1999). Three MAP kinases, p44/p42 MAP kinase, p38 MAP kinase and stress-activated protein kinase/c-*Jun* N-terminal kinase (SAPK/JNK), are known as central elements used by mammalian cells to transduce the various messages (Widmann et al., 1999). It has recently been reported that IGF-I up-regulated expression of core binding factor α1 through MAP kinase pathway in osteoblast-like MC3T3-E1 cells (Pei et al., 2003). However, the exact role of the MAP kinase superfamily in IGF-I-effect on osteoblasts has not yet been clarified.

In the present study, we investigated whether the MAP kinase superfamily is involved in the IGF-I-induced alkaline phosphatase activity in osteoblast-like MC3T3-E1 cells. We here show that IGF-I activates p44/p42 MAP kinase and p38 MAP kinase in these cells, and that p44/p42 MAP kinase plays a part in the IGF-I-stimulated alkaline phosphatase activity.

2. Materials and methods

2.1. Materials

IGF-I was purchased from R&D Systems, Inc. (Minneapolis, MN). Specific inhibitors for MEK (PD98059 and U0126), p38 MAP kinase (SB203580 and PD169316) and phosphatidylinositol 3-kinase (PI3K) (LY294002 and wortmannin) were obtained from Calbiochem-Novabiochem Co. (La Jolla, CA). Phospho-specific p44/p42 MAP kinase antibodies, p44/p42 MAP kinase antibodies, phospho-specific p38 MAP kinase antibodies, p38 MAP kinase antibodies, phospho-specific SAPK/JNK antibodies and SAPK/JNK antibodies were purchased from New England BioLabs, Inc. (Beverly, MA). ECL Western blotting detection system was purchased from Amersham Japan (Tokyo, Japan). Other materials and chemicals were obtained from commercial sources. PD98059, U0126, SB203580 and PD169316 were dissolved in dimethyl sulfoxide. The maximum concentration of dimethyl sulfoxide was 0.1%, which did not affect assay for alkaline phosphatase activity or the analysis of MAP kinases.

2.2. Cell culture

Cloned osteoblast-like MC3T3-E1 cells derived from newborn mouse calvaria (Sudo et al., 1983) were maintained as previously described (Kozawa et al., 1992a). Briefly, the cells were cultured in α-minimum essential medium (α-MEM) containing 10% fetal calf serum (FCS) at 37 °C in a humidified atmosphere of 5% CO_2/95% air. The cells were seeded into 35-mm diameter dishes or 90-mm diameter dishes in α-MEM containing 10% FCS. After 5 days, the medium was exchanged for α-MEM containing 0.3% FCS. The cells were used for experiments after 48 h.

2.3. Assay for alkaline phosphatase activity

The cultured cells were pretreated with PD98059, U0126, SB203580 or PD169316 for 60 min, and then were stimulated by IGF-I in 1 ml of α-MEM containing 0.3% FCS for the indicated periods. At the end of the incubation, the cells were harvested by scraping with a rubber policeman into 1 ml of 0.2% Nonidet P-40 and disrupted by sonication. After centrifugation at 1500 × *g* for 5 min of the homogenate, alkaline phosphatase activity of the supernatant was measured by the method of Lowry et al. (1954).

2.4. Analysis of mRNA expressions

The cultured cells were stimulated by IGF-I or vehicle in α-MEM containing 0.3% FCS for 0, 12, 24, 36, 48 and 60 h. The expression levels of mRNAs were estimated by semi-quantitative reverse transcription-polymerase chain reaction (RT-PCR) according to the method previously described by Nakashima et al. (2005) and Ishisaki et al. (2004). In brief, at the end of each incubation period, the total RNA was extracted from the cells using Isogen (Nippongene, Toyama, Japan) and complementary DNA was synthesized with Omniscript reverse transcriptase (Qiagen, Valencia, CA) using an oligo$(dT)_{15}$ primer (1 μM) according to the manufacturer's instructions. Each PCR reaction was carried out in 50 μl of mixture containing 1 μl of cDNA, 5 μl of 10× Qiagen PCR buffer, 10 μl of 5× Q-solution PCR buffer, 1 μl of 10 mM each deoxynucleotide triphosphate mix, 0.1 μM each sense and antisense primers and 0.25 μl of Taq DNA polymerase (Qiagen). Each reaction consisted of initial denaturation at 94 °C for 3 min followed by three-step cycling: denaturation at 94 °C for 30 s, annealing at a temperature optimized for each primer pair for 30 s, and extension at 72 °C for 1 min. Amplification was stopped within linear range and the reaction underwent a final extension at 72 °C for 10 min. Twenty-five cycles were undergone. Amplification products were electrophoresed on 1.2% agarose gels and visualized by ethidium bromide staining followed by UV light illumination. Equal loading of RNA samples were checked by amplification of GAPDH cDNA. The primer sequences used for PCR amplifications, annealing temperature, and expected fragment size were as follows: osteocalcin, forward primer 5′-CTGAGTCTGACAAAGCCTTC-3′, reverse primer 5′-GCTGTGACATCCATACTTGC-3′, 55 °C and 312 bp; osteopontin, forward primer 5′-CGACGATGATGACGATGATGAT-3′, reverse primer 5′-CTGGCTTTGGAACTTGCTTGAC-3′, 60 °C and 495 bp; Runx2, forward primer 5′-AGCAACAGCAACAACAGCAG-3′, reverse primer 5′-GTAATCTGACTCTGTCCTTG-3′, 55 °C and 470 bp; collagen α1(I), forward primer 5′-TCTCCACTCTTCTAGTTCCT-3′, reverse primer 5′-TTGGGTCATTTCCACATGC-3′, 51 °C and 269 bp; glyceraldehydes-3-phosphate dehydrogenase (GAPDH), forward primer 5′-TTCATTGACCTCAACTACATG-3′, reverse primer 5′-GTGGCAGTGATGGCATGGAC-3′, 60 °C and 443 bp, respectively.

2.5. Analysis of MAP kinases

The cultured cells were stimulated by IGF-I in α-MEM containing 0.3% FCS for the indicated periods. The cells were washed twice with phosphate-buffered saline and then lysed, homogenized and sonicated in a lysis buffer containing 62.5 mM Tris–HCl, pH 6.8, 2% sodium dodecyl sulfate (SDS), 50 mM dithiothreitol and 10% glycerol. The cytosolic fraction was collected as a supernatant after centrifugation at 125,000 × *g* for 10 min at 4 °C. SDS-polyacrylamide gel electrophoresis (PAGE) was performed by Laemmli (1970) in 10% polyacrylamide gel. Western blotting analysis was performed as described previously (Kato et al., 1996) by using phospho-specific p44/p42 MAP kinase antibodies, p44/p42 MAP kinase antibodies, phospho-specific p38 MAP kinase antibodies, p38 MAP kinase antibodies, phospho-specific SAPK/JNK antibodies or SAPK/JNK antibodies with peroxidase-labeled antibodies raised in goat against rabbit IgG being used as second antibodies. Peroxidase activity on the nitrocellulose sheet was visualized on X-ray film by means of the ECL Western blotting detection system. When indicated, the cells were pretreated with PD98059, U0126, PD169316, LY294002 or wortmannin for 60 min.

2.6. Determinations

The absorbance of enzyme immunoassay samples was measured at 450 nm with EL 340 Bio Kinetic Reader (Bio-Tek Instruments, Inc., Winooski, VT). The densitometric analysis was performed using Molecular Analyst/Macintosh (Bio-Rad Laboratories, Hercules, CA).

2.7. Statistical analysis

The data were analyzed by ANOVA followed by the Bonferroni method for multiple comparisons between pairs, and a $p < 0.05$ was considered significant. All data are presented as the mean ± S.E.M. of triplicate determinations. Each experiment was repeated three times with similar results.